FILE

James Rennell Centre
for Ocean Circulation

INTERNAL DOCUMENT No. 13

Industrial Training Year at the James Rennell Centre for Ocean Circulation: 16 Aug 1992 - 27 Aug 1993

S K Ward

1993

UK
WOCE

Institute of
Oceanographic Sciences
Deacon Laboratory

Natural Environment Research Council

JAMES RENNELL CENTRE FOR OCEAN CIRCULATION

INTERNAL DOCUMENT No. 13

Industrial Training Year at the James Rennell Centre for Ocean Circulation: 16 Aug 1992 - 27 Aug 1993

S K Ward

1993

Gamma House
Chilworth Research Park
Chilworth
Southampton SO1 7NS
Tel 0703 766184
Telefax 0703 767507

INTRODUCTION

The Importance of Ocean Circulation

Oceanography as a science is widely regarded to have begun with the voyage of the *RRS Challenger* from 1872 to 1876. This was the first voyage with purely scientific motives. Before this, exploration of the oceans was geared towards charting waters so that trading vessels could use prevailing winds and currents to speed their passage. Ports and harbours were sounded for shoals and rocks, and the sea bed was examined to discover the best routes for laying telegraph cables. The *Challenger* was commissioned to observe the biological, chemical, geological and physical processes in the ocean as it circumnavigated the globe. This gave the first general description of the ocean's character.

During the twentieth century, the emergence of the submarine as a major force in national defence was the impetus for much research and development of new instruments to learn more about the under-sea environment. The vast resources of the sea, both biological and mineral, were strong economic factors influencing the growth of oceanography.

In recent decades it has become clear that man's activities are having an effect on the world around us. The increased concentration of Carbon Dioxide in the atmosphere since the Industrial Revolution is well documented, and the discovery of the hole in the Ozone layer in 1986 demonstrated that these effects can be damaging.

The oceans are an integral part of the world's climate system. Solar energy is absorbed at the Tropics and transported pole wards at the sea surface. The cooler water from the poles sinks down into the deep ocean and flows towards the equator. This process, known as thermohaline circulation, transports billions of megawatts of heat towards the poles. The winds driving the ocean redistribute heat around ocean basins, affecting regional climate and rainfall patterns, and generate major currents such as the Gulf Stream. The oceans have a huge heat capacity and act as a buffer to any atmospheric temperature rises.

Atmospheric monitoring and forecasting is now an everyday occurrence, with meteorologists able to predict regional weather several days in advance. The use of atmospheric modelling to predict long term climate change is impossible without taking into account the effect of the oceans. There are, however, large gaps in our knowledge of ocean processes. As part of the World Climate Research Programme, the World Ocean Circulation Experiment (WOCE) is being undertaken by over forty countries. This will try to fill in those gaps by taking a global snapshot of the oceans, using this to develop numerical models of the ocean, and coupling these with atmospheric models. It is a fore-runner to the Global Ocean Observing System, a future project for the operational monitoring of the oceans using satellites, ships and buoys. The prediction of the time scale and regional effects of climate change would then be possible to a much higher degree of accuracy than is currently possible.

The James Rennell Centre for Ocean Circulation

When the Natural Environmental Research Council (NERC) was formed in 1965 its purpose was to bring together all the different environmental agencies under the management and funding of one central body. The National Institute of Oceanography was formed at this time. Sited at Wormley in Surrey, it combined with the Institute of Coastal Oceanography and Tides and the Unit of Coastal Sedimentation in 1973, to become the Institute of Oceanographic Sciences Deacon Laboratory (IOSDL). In 1990 the James Rennell Centre was set up by NERC at Chilworth in Southampton, as part of IOSDL, to co-ordinate the UK's contribution to WOCE. The James Rennell Centre is now managed independently to IOSDL, and so together these form the Institute of Oceanographic Sciences as it is today. 1995 will see the completion of a new dockside centre at Southampton, into which will go IOSDL, the James Rennell Centre, Southampton University Department of Oceanography and Research Vessel Services (currently situated at Barry in South Wales).

The James Rennell Centre is organised around six scientific teams. The Tracer Chemistry team examine water samples for concentration of key tracers such as oxygen and CFCs to identify water masses and determine their "age" i.e. when they were last at the surface. The role of the Survey team is to collect hydrographic data from the areas considered important to WOCE and provide initial scientific interpretation of the data. The Modelling team develop feature models, mathematical descriptions of well-mapped physical processes, and the Atlantic Isopycnic Model which uses surfaces of constant density to predict the behaviour of the Atlantic Ocean. The Biological Modelling team are constructing Carbon flux models, studying the effect of phytoplankton growth and the Carbon cycle on Carbon Dioxide concentration in the atmosphere. The Satellite and Remote Sensing team are conducting research into extracting oceanographic measurements from altimeter scatterometer and radiometer data, such as wave height and surface wind speed. The Surface Fluxes team use data from ships, buoys and satellites to evaluate fluxes of heat, momentum and moisture, and improve the scientific understanding of the processes that govern these transfers.

Each week the head of centre holds an informal discussion during the coffee break, where recent managerial decisions can be explained and the latest news announced. The centre has an internal seminar programme, where work mates present an informal talk at lunch time on their current projects. These are informative and maintain an general idea of what other research is being undertaken at the centre. Visiting scientists from other establishments around the world are frequently asked to give more formal presentations, which attract many of Britain's top oceanographers. The scientific discussion which follows can be lively and educational.

Report Layout

The following section describes the experience I have gained from spending a year working at a Research Institute. The third section reproduces the report prepared for my supervisors on my main project for the year, the effect of waves on the drag coefficient of the open ocean. This goes into sufficient detail about file names, program descriptions, processing routes and instrumentation corrections to enable the work to be extended for publication at a later date.

EXPERIENCE

Computing Facilities at the JRC

The centre has a Ethernet network linking several Sun workstations, and each individual has an Apple Macintosh which acts as a terminal. There are also two Silicon Graphics machines which are used to run data visualisation packages. Each team has its own server, linked to a UNIX operating system. This spreads the load on the system, and speeds up data access time. The system is supported by a data storage device called an Epoch. The Epoch works as an optical jukebox, storing unused data to optical disc, and holding recently accessed files on a magnetic disc. The capacity of the Epoch is in the region of 80 GBytes, all of which is more or less instantly accessible to anyone who needs it. The system is maintained by two on site NERC Computer Services personnel.

UNIX operating system

As Bath University uses a similar system, I was familiar with basic UNIX commands and the directory structure. I have gained considerably more knowledge of how the system operates, and the workings of a distributed network. My initial work was to process several cruises' worth of Ship Borne Wave Recorder data from the O.W.S. Cumulus, and it soon became obvious that this involved running the same programs repeatedly for each data file, with similar inputs. I simplified the process by creating a script called SurfsUp. It requires the user to provide two files, then one operation of the script performs all the processing that is needed to correct and smooth the spectral data ready for plotting, and calculate a wave height from the information. SurfsUp is shown as a flow chart in Fig 1.3. I also produced scripts to process Propeller anemometer data, send files to printers, change the format of Met office files, and to do various other tasks that would have to be performed on a large number of files

Pexec System

The Pexec, or pstar, system is a library of Fortran programs, all constructed from a suite of data handling subroutines. The pstar format was devised at IOS to handle the large amounts of time series data collected during research cruises. Pstar is a self-describing system, each file has a header which contains information as to the number of variables and data cycles in the file, variable names and units, and where the data came from. The pstar programs read this header information, and can therefore deal with any type of data, and any number of variables.

The pstar program library is fairly extensive, containing over 200 programs to perform various functions. If you wish to perform a function not catered for in the library, skeleton programs are provided that can be customised to your requirements. Owing to the wide variety of tasks I had to perform in the course of my project, it was frequently necessary to generate new programs. Occasionally, the skeleton programs provided were not suitable for my needs, so I built the

programs from scratch in a more logical structure. The programs developed for use in my project are given in an inventory in Section 1.3 of the project report.

One task was to examine an existing on-screen editing program, *plxyed*, to increase its efficiency, as I would be using it regularly, and its run-time seemed unnecessarily long. Taking a complex graphics program that works and looking for the areas in the code where it was inefficient required an understanding of how the various functions were being performed at microprocessor level. The reason for the slow operation of the program was a result of its general nature, creating and searching through large arrays, which was not necessary when examining time series data. By making the program specific to time series data I was able to produce a speedier version, *pltyed*.

As a result of this I have gained considerable programming experience in Fortran, both in the use of the language and in the efficient structuring of programs.

Packages

The JRC supports a wide variety of packages, both on the Suns and on the Apple Mac's. On the Mac's I have had considerable experience with Microsoft Word 5.1 (word processing), Cricket Graph (data display), MacFlow (flow chart creation), MacDraw Pro (graphics) and Microsoft Excel (spreadsheet). I have also used Systat (statistics), and Adobe Photoshop (high definition graphics) in conjunction with a colour scanner.

On the Sun or the Silicon Graphics machines the most commonly used package is Unimap. The centre also has PV-Wave, Vis-5D and Explorer. One of the major problems with most of these packages is actually getting your data into them in a recognisable form. To evaluate its usefulness to the Met team, I familiarised myself with PV-Wave. The main aim was to see if a general Pstar-to-PV-Wave conversion program could be created. The conclusion was that owing to the type of work the Met team does, the effort involved far out-weighed the advantages the package had over the familiar pstar library in most situations.

Data processing/analysis

During my year at the James Rennell Centre I have had experience in almost every stage of data collection, processing, analysis and presentation. The opportunity did not arise to participate in a research cruise, however, I was able to travel to Greenock near Glasgow to visit the O.W.S. Cumulus at one of its port calls. The majority of the instrumentation had been removed a few cruises earlier, as the ship went in to dry dock for a refit, and had to be replaced in the day and a half the ship was in port. I assisted in the down-loading of data from the Ship Borne Wave Recorder (SBWR) PC, and reinstallation of the Multimet Logger and GPS systems. I was also volunteered to replace the Solent sonic anemometer at the top of the ship's mast.

Commissioned Research Reports

The Met team is part-funded by Commissioned Research Projects. These occasionally involve providing meteorological data for research cruises being undertaken by other institutions. The Woods Hole Oceanographic Institute (WHOI) commissioned data from the R.R.S. Charles Darwin Cruise 73, which took place in September/October 1992. The Instrumentation group of the Met team handled the deployment of the Multimet logger and instruments before the cruise, and the down-loading of data and demobilisation of equipment afterwards.

I was given the job of transferring the data onto the JRC Sun system, despiking and analysing it to detect any calibration errors in the instruments. Once this was done I prepared a document on the complete project, bringing together the reports of the scientists who deployed and retrieved the data and instruments, along with my own analysis of the quality of the data. This was published as a JRC internal document (S Ward *et al.* 1993) and was sent with the data to WHOI. The analytical skills acquired during this work proved valuable in the processing of the O.W.S. Cumulus data set, and with my main project for the year.

Data Management

Owing to the large amount of data involved with the O.W.S. Cumulus, it is vital to keep a record of what data is where, and the state of the processing. As well as simplifying a lot of the work by writing scripts, I helped to develop a standard processing and storage procedure, laying out what must be done to each of the various data sets: GPS, turbulence, slow sampled and SBWR. This is to be published as a JRC internal document, and will make it possible for anyone to perform the required processing with no previous knowledge of the Cumulus data set.

As my work this year involved a large amount of data processing and analysis, I created a great number of working files. An up-to-date log book became essential to my work, to keep track of the programs that had been run on the various files, and to store plots of the data at different stages.

Presentation of Work

As well as the talk given at Bath in February, I and my two fellow Industrial Training Students were each asked to present a 15 minute talk about spending a year at the James Rennell Centre, as part of the internal seminar program. The task of presenting the results of my project to my work mates was a daunting one. I found a major problem was deciding what to leave out, as 15 minutes is a very short time in which to present a year's work. I had to examine the reasoning behind the different areas of the project, and look at what the most important parts were, which were not necessarily the ones that had taken the most time, or the ones I had enjoyed most. The discussion following the talk provided some interesting ideas from people who had worked in similar areas in the past, and had experience of the problems involved. This demonstrated the usefulness of open discussion with people who aren't necessarily the obvious people to approach with a particular problem.

Working Environment

The Met Team

The Met team is split into two groups, the Instrumentation group at IOS Deacon Lab, and the data analysis group at the JRC, of which I was a part. The data analysis group is a four-man team, the industrial training student included. As part of this small group, I found that initially I relied heavily on the other members for help when I had problems with my work, or with the computing system. It took some months for me to gain enough experience and confidence to present my own ideas and opinions. An important aspect of this was being able to explain why I held these opinions, or why I thought that something should be done one way rather that another, and to present data to back up my views. I regularly had to explain my work to my supervisors, especially while formulating the corrections for the motion of the O.W.S. Cumulus, (Section 3.4 in the project report) as little was known about this at the time.

The James Rennell Centre

The JRC is an open-plan building, which promotes communication and a relaxed atmosphere. It is easy to approach people with work difficulties, and also to help out if someone is obviously struggling with a particular machine, or problem. The internal seminar programme provides a means of informing the rest of the centre about the work being done in each department, and in which areas other teams are concentrating.

There are a number of regular sporting/social activities such as football, volleyball and rounders going on, which are good fun and generate a friendlier atmosphere at work. It was my experience that a discussion over a pint could provide a far more interesting view of another's work than if the discussion took place during working hours.

CONCLUSIONS

During the year I have spent at the James Rennell Centre I have been given the opportunity to work as a member of a scientific team. I feel I have been shown what it would be like if I was a full time employee and have come to appreciate the long time scale over which research progresses. I have met and spoken to a great many scientists at all levels of management, at coffee breaks, attending seminars and while travelling to other institutes, and have been given a clear view of the workings of a strategic research centre. I have gained an insight into how experiments are set up and funded and how the research centres themselves are run. I have also seen for myself the frustrations and rewards that accompany a career in science.

THE EFFECT OF SEA STATE ON THE DRAG COEFFICIENT

1.1: Introduction

The Surface Fluxes team use data from ships, buoys and satellites to evaluate the momentum, heat and moisture fluxes at the sea surface, and to improve the understanding of these fluxes. The identification of key parameters influencing the processes involved enables boundary layer models to be created and tested. These can then be used as boundary conditions for ocean climate models.

The momentum transfer between the atmosphere and the sea, wind stress, is a function of the turbulence in the air, but can be related to the mean wind field via the drag coefficient of the ocean. Measurements of this parameter suggest its value changes in different locations, it varies with wind speed and with sea state.

This report details the work completed in studying the effect of waves on the drag coefficient of the open ocean. A brief theory of wind stress is given in Section 1.2, followed by an inventory of programs and scripts written during the course of the project in Section 1.3. Section 2 describes the examination of turbulence data from the R.R.S. Charles Darwin and evaluation of a response correction for propeller anemometers. The work involved in processing and analysis of the Ocean Weather Ship Cumulus data set is described in Section 3. Section 4 details the analysis of data from the R.R.S. Discovery SWINDEX Cruise 201.

1.2: Theory

In the lowest 50 m of the atmosphere the wind stress is regarded as being independent of height (depending on stability). Wind stress is defined as the vertical transport of horizontal momentum between the air and the sea:

$$\tau = -\rho\langle uw \rangle$$

where the brackets denote a time average of u and w, the along and vertical wind speed fluctuations.

In this layer, a friction velocity, u*, may be defined by:

$$u*^2 = \tau / \rho$$

where ρ is the air density. Wind stress can be related to the mean wind speed, U, relative to the sea surface via the Drag Coefficient, CD:

$$u*^2 = CD\, U^2$$

This is known as the Bulk Aerodynamic Formula.

The Drag Coefficient is thought to have a linear dependence on wind speed of the form:

$$CD = a + b\, U$$

The graph in Fig 1.1 reproduces a summary of recent studies into the value of the Drag Coefficient (Geernaert, 1990). The range of values for a and b is broad, and the individual studies have a large amount of scatter in their data. It is generally accepted that this scatter is due to the presence of other variables which affect the Drag Coefficient, particularly sea state.

1.3: Program inventory

In the course of the project it was necessary to develop new scripts and Pexec programs for the different stages. These are listed here with a brief description of their function.

deltawind - Calculates the change in the wind vector with time. The program outputs rate of change of magnitude, direction, and along- and across-wind components per unit time. The components are relative to the original wind direction, but assigned to the new wind speed and direction values. This is shown schematically in Fig 1.2.

distcalc - Takes a gridded spectral Pstar file as input, with frequency, wind speed and log10PSD variables, and outputs a non-gridded file of three distance constant values for each spectra over three different frequency ranges. These ranges can be altered in the data statements at the start of the program.

fslcum - This is a copy of the Pexec program *fslpond* to calculate drag coefficient values. The version *fslcum* has the correct instrument heights for the Cumulus in it (24m for anemometer, 12m for psychrometers).

fsldisc - A copy of the Pexec program *fslpond* with the correct instrument heights for the Discovery (13.5 m for anemometer, 17 m for psychrometers).

fsneucum - As *fslcum* but with assumed neutral stability i.e. no stability corrections.

metfluxd - This is a copy of the Pexec program *metflux* to predict friction velocity values from bulk formulae. The equation relating the drag coefficient to the mean wind speed is that derived from the Discovery Cruise 201 data.

pltyed - This program is an edited version of the Pstar program *plxyed*, made more efficient by converting the code to apply to time series data only.

rescor1m/rescor2m - Takes gridded spectral Pstar file of psd values and outputs PSD*$F^{5/3}$ after applying a response correction to the data. This program also applies corrections for binning factors and missing calibrations in the subroutine 'ressub'. The distance constant value used is set in a data statement.

SurfsUp - Script to read in spectral data files in ascii format from the Ship Borne Wave Recorder into Pstar format. This script corrects the data for instrument response, selects a frequency range of values, and smoothes the data ready for contour plotting. It also calculates the significant wave height from the spectra, and outputs this to a separate file. The programs run by the script are shown in the flow chart in Fig 1.3.

windcor/windcors - A correction for ship's speed is applied to the relative wind variable as function of relative wind speed and direction. The first output variable is true wind. The way the data is treated (i.e. hove-to, port or other) is indicated by the second output variable (called 'modus' with 'operandi' as units) where a value of 1 is hove-to, 2 is port drift and 3 is any other wind

direction. This is done in the subroutine 'windsub' by selecting for wind directions between appropriate ranges. The program *windcors* outputs calculated ship's speed, as well as true wind and m.o., as the third output variable.

Youngscrp - Script to read in ascii spectral data files from a fast sampled propeller anemometer into pstar format. Input files are the output from the program *fftcopy* on the Archimedes.

2: R.R.S. Charles Darwin Cruise 43

2.1: Introduction

This cruise took place in October and November of 1989 in the region of the Faeroe Islands to the North of Scotland. One of the aims of the IOSDL Meteorology group, in conjunction with the University of Manchester Institute of Science and Technology, was to investigate the transfer of momentum in high wind speed conditions and changing sea state. Several anemometers were employed in close proximity to each other to evaluate differences between the various instruments. These included a Young propeller vane of the type deployed on the O.W.S. Cumulus, and a Kaijo Denki sonic anemometer (Taylor *et al.* 1991).

The data from this cruise had been processed and the performance of the different anemometers compared as part of paper submitted for publication in the Journal of Atmospheric and Oceanic Technology (Yelland *et al*). The Young propeller raw data was available on 5.25" floppy disc, the same format as the data from the O.W.S. Cumulus. The data was re-processed in the same way as is necessary for the O.W.S. Cumulus data, then compared to the original data to assess the validity the different processing route. Once this was done the frequency range over which the average power spectral density (PSD) and propeller distance constant are calculated was investigated to see if an improvement could be made in the comparison with the sonic anemometer.

2.2: Data Processing Route

The processing route used for the Charles Darwin data set is shown in Fig 2.1. The program *fftcopy* on the Archimedes reads off the spectra from 5.25" floppies and stores them in ascii files. These are transferred onto the Sun by way of 3.5" floppy and the Mac. *Youngscrp* is used to read in all the files for one cruise into a pstar file with 80 grids. The files have one spectra every 18 minutes of which 10 minutes 40 seconds is spent data sampling and the remainder is spent calculating the spectra and writing them to disk. The variables in the file are jday, frequency and $\log_{10}$PSD. The multimet data is put on to this file in the following manner: the first row of jday is copied into another file using *pcopyg* , and *minmid* is used to average the phydata variables onto this time base. Values of zero minutes before and 10 minutes after the times in the first file are used. Then *pmerg2* is used to put these variables onto the original gridded psd file. As the time bases are identical there is no interpolation.

The data was selected for winds on the bow only (relative wind direction between 160° and 200°) then the distance constant was calculated between 1 and 2 Hz using the program *distcalc*. The values for the distance constant are shown against wind speed in Fig 2.2. The average value between 8 and 12 m/s was found to be 0.81 m. This value was used in *rescor1m* to calculate $PSD*F^{5/3}$. The subroutine *ressub* was altered to multiply the PSD value by several factors that were either missing in the original BBC Basic logging program or resulting from incorrect calibration of the instrument. These values are:

Wind Speed * 0.9739	wrong calibration
PSD * 0.9739^2	wrong calibration
PSD * 64	Converts spectral value to Power Spectral Density
PSD * 1.5	Due to incorrect calculation of windowing correction in original logging program.

N.B. Only the factors of 64 and 1.5 are needed in the Cumulus processing.

2.3: Data Analysis and Results

The data was examined to determine the inertial sub-range, the region with a $(frequency)^{5/3}$ tail, over which the PSD is averaged. In this range the gradient of $PSD*F^{5/3}$ when plotted against frequency is zero. The range used in the original processing was 1 to 2 Hz.

The average $PSD*F^{5/3}$ was taken between 0.8 Hz and 2.2 Hz for each spectrum then subtracted from the spectrum at each frequency. The difference between the mean and the measured $PSD*F^{5/3}$ values for all the spectra were binned into frequency ranges. Fig 2.3 shows the normalised spectra are flat in the region 1 Hz to 1.8 Hz.

Distcalc was altered to calculate the distance constant over this range, and it was again found to be 0.81 m. The complete data set was corrected using this value, then the average $PSD*F^{5/3}$ was calculated over the range 1 to 1.8 Hz. The data was compared to that from the Kaijo Denki sonic anemometer in the same manner as previously done by Yelland. These comparisons are shown in Fig 2.4. The Young propeller vane is giving a uniformly higher value for the PSD than the Kaijo Denki for all wind speeds. In the original processing the propeller gives lower values of PSD for wind speeds below 10 m/s, then higher values for PSD than the Kaijo Denki for wind speeds above 10 m/s. The use of a lower distance constant and smaller frequency range has therefore improved the comparison with the sonic anemometer. The file containing the original sonic anemometer and Young data, and the reprocessed Young data is named 'cd43anemoms'. Its header is shown in Fig 2.5.

3: O.W.S. Cumulus Data

3.1: Introduction

The Ocean Weather Ship Cumulus is owned by the Meteorological Office, and is one of two remaining weather ships still in operation. In the 1950's there were a dozen or so ships owned by the countries that surround the North Atlantic, as a result of the Ocean Weather Ship Agreement. This called for each country to deploy a stationary meteorological ship in a certain area (Hatch, 1993). The purpose of these ships was to take surface meteorological readings and release radiosonde balloons to enable aeroplanes to be informed of weather conditions. The weather ships also tracked the trans-Atlantic flights using radar, to update the gyro position systems used by the planes, which tended to drift. The advent of satellites and satellite meteorology succeeded the capabilities of the weather ships in both accuracy and coverage, so the Ocean Weather Ship Service was gradually reduced.

The O.W.S. Cumulus is situated at Station Lima, an area of around 10 square miles centred at 57°N 20°W. The ship holds station for four weeks in every five, returning to Greenock near Glasgow to refuel and take on supplies each month. The Met team has had instrumentation deployed on the Cumulus since 1987, providing a long time series of data from the open ocean in varied and sometimes extreme weather conditions.

3.2: Instrumentation

The instruments deployed on the Cumulus vary from cruise to cruise depending on availability and man-power. The instrumentation, quality and processing state of the Cumulus data set, up to November 1992, is summarised by Taylor *et al* (1992). The instruments concerned with this project are:

A Multimet logger taking one-minute averages of 1 Hz sampled meteorological data (wet and dry air temperatures, air pressure, wind speed and direction), a fast-sampled Young Propeller vane providing turbulence spectra, deployed for several cruises before being replaced with a sonic anemometer, the recently installed Global Positioning System giving one-minute values of position over the ground, and a Ship Borne Wave Recorder providing non-directional wave spectra every 15 minutes.

3.3: Routine Data Processing

Data from the Multimet Logger is removed from the ship on tape cartridge in raw ascii format. This is transferred onto JRC Sun system, then converted into pstar format. Calibration equations and coefficients are applied to the various channels depending on the instruments used. Once in physical units, the data can be examined and despiked. This process is shown in the flow chart in Fig 3.1, giving the names of the pstar programs used at each stage.

The Ship Borne Wave Recorder writes out spectral data to a file every ten minutes. For each cruise, there are several hundred files. These are read into pstar format in 10-day sections, giving 4 or 5 files per cruise. Once in pstar format, the data is corrected for sensor response, smoothed and gridded ready for contour plotting. A significant wave height (defined as the average height of the largest third of the waves) is calculated by performing an integral of spectral energies over a frequency range 0.04 to 0.99 Hz. The processing route is shown in Fig 3.2.

The flow chart in Fig 2.1 shows the processing route used for the Young Propeller turbulence data as described in Section 2.2.

Anemometer Orientation

The despiking process includes setting the relative wind direction so that 180° refers to wind directly on the bow. Histograms of relative wind direction for cruises where the Young Propeller Vane was deployed suggested that this was not the case. The Young anemometer had been aligned on the ship, however the zero point on the potentiometer used to measure wind direction was not in line with the zero mark on the casing of the instrument. A comparison of peaks in relative wind direction between cruises with Young data and those where the Solent sonic was deployed was made, to determine the exact offset of the wind vane. Tables 3.1 (Young cruises) and 3.2 (Sonic cruises) show the peaks in the relative wind direction histograms which apply to hove to and port drift for each cruise, and give an indication of the proportion of the cruise for which the ship was hove to. The histograms of relative wind direction for cruise 70 to 77 are shown in Fig 3.3.

The mean relative wind direction referring to port drift from cruises with the sonic anemometer is 93°. The hove to peak averages at 173° for cruises 70 and 76, which have a small proportion of hove to data, and 180° for cruises 71 and 72, where the ship was hove to for a large proportion of the cruise. For the cruises with the Young propeller, the mean port peak is at 69°. For those cruises with a small amount of hove to data, the hove to peak is at 158°. The cruises with large amounts of hove to data have an average peak at 165°. This information suggests an offset of 21° brings the Young vane into alignment to within 2° of the bow. This has been applied to the despiked multimet data.

3.4: Corrections for the ship's motion

Introduction

Navigation and wind speed data from the O.W.S. Cumulus has been examined with the following aims:-

a) To determine the most effective smoothing interval for the GPS data.

b) To investigate the possibility of a direct relationship between the ship's speed and the relative wind speed when the ship is drifting. If a relationship can be found, it may reduce the errors involved in using hourly navigation data to calculate true winds for cruises for which there is no GPS data.

The O.W.S. Cumulus has a pattern of behaviour while at Station Lima, knowledge of which is important for understanding data received back at the JRC. The ship spends as much time as possible while it is on station drifting on a port tack (that is port side to wind) so that the IOS meteorological instrumentation on the ship is advantageously exposed to the air flow. If the weather becomes too rough to safely maintain this drift, then the ship steams slowly into wind to ride out the storm. If the ship's drift takes it to the edge of the station, then it steams back to the other side and continues drifting port beam to wind.

Data available for the study

The data needed for each cruise is:

a) GPS navigation data, giving one minute values of position

b) Wind speed and direction data from the sonic anemometer, sampled at 1 Hz and averaged to give one minute values.

The GPS system was installed on cruises 63 to 65, and cruise 70 onwards. The ship was struck by lightning on cruise 62 which meant that no wind data was available for the next three cruises. At this point all instrumentation was removed as the ship was going into dry dock for a refit. The instruments were replaced prior to cruise 70, however, because of a faulty connection in the anemometer lead on cruise 73 and the failure of the GPS system on cruise 74 which required its removal to be repaired during the next cruise, concurrent wind and GPS data is available for cruises 70, 71, 72, 76 and 77 only.

The histograms in Figs 3.4 and 3.5 show the number of one-minute observations taken at each wind speed when the GPS system was in Navigation mode. Fig 3.4 shows data collected when the ship was drifting, hove to data is shown in Fig 3.5. The histograms suggest that the ship does not maintain a port drift above wind speeds of 17 m/s. The lowest wind speed at which the ship heaves is 12 m/s. The percentage of time the ship spends drifting or hove to as a function of wind speed is shown in Fig 3.6. This suggests that above wind speeds of 17 m/s, the ship is hove to for 95% of the time. Below wind speeds of 12m/s the ship drifts for 90% of the time, between 12 and 17 m/s the ship may be either drifting or hove to.

GPS Data Filtering

The GPS position data has the characteristics of a low frequency signal surrounded by higher frequency noise. This noise produces errors in the calculated ship's speed and direction. The response of the filter used must be such that it allows the signal through in as much detail as possible while stopping the noise from passing through. It was decided to use a 'top hat' filter, i.e. each data point is the average of a number of equally weighted points on each side, and the effect of using different numbers of points was examined for Cruise 71 GPS data.

Initially, the position data was selected for when the system was in Navigation mode. This was smoothed using filter lengths of 3,5,7,9,...,27 and 29 points, and the ship's speed calculated for each data set produced. The Pstar program *parith* was used to find the difference between the speed calculated from the original data set and that from the various filtered ones. Fig 3.7 shows the standard deviation of this difference against the number of weights used in the filter. The

number of points taken in the average for each individual point is two times the number of weights plus one. The plot shows that the optimum number of weights to use in the filter is six, (a 13-point average) as this is the point at which the standard deviation of the mean difference reaches a plateau. Fig 3.8 shows a 3.6 hour sample of GPS data, comparing ship's speed calculated from unfiltered positions with ship's speed calculated after the positions have been filtered using the 13-point average.

Data Processing

As stated above, for the purpose of this study concurrent wind data and GPS data is needed. The two are logged on separate machines, the wind data from the sonic anemometer by the Multimet Logger (Birch *et al.* 1993), and the GPS navigation data on a PC. As a result of this each data set is in a separate file, with the time bases out of sync. It is also important to note that once the GPS data has been selected for Navigation mode only, the time base is no longer continuous, with jumps where the GPS was not navigating for any period of time. If the GPS data is interpolated onto the wind data, these gaps are filled with interpolated data, which would clearly lead to inaccuracies in any wind speed/ship's speed relation produced. For this reason the wind data must be interpolated onto the GPS data. The wind data must be in component form, i.e. U and V components from the sonic anemometer. If speed and direction variables are used, direction changes from 0° to 360° may be interpolated to 180°.

The data from each cruise was processed in exactly the same way, so that the results would be comparable. The flow chart in Fig 3.9 shows the processing route, and gives the names of the Pstar programs used to perform each step. Once the wind data had been interpolated onto the GPS data, the GPS data was filtered to remove any scatter. The ship's speed, direction, and vectors East and North were calculated, then the wind vectors U and V were converted to wind speed and direction. The sonic anemometer is not in line with the ship, so the relative wind direction must be increased to assign a relative wind direction of 180° to wind directly over the bow. This value is 30° for cruises 70, 71 and 72 and 120° for cruises 76 and 77. This was then corrected to between 0° and 360°. It is useful to examine the speed in its component parts, velocity in the fore/aft direction and velocity in the port/starboard direction.

These components are given by:-

$$S_f = S \cos \theta$$

$$S_s = S \sin \theta$$

$$(\theta = Shipdir - Heading)$$

where Sf is defined positive when the ship moves forward and Ss is defined positive when the ship moves towards its starboard side. Shipdir is the direction the ship is travelling, and Heading is the direction the ship is pointed.

The heading was corrected for the magnetic variation of the North Pole, which was 15.6° at Station Lima around the times of cruises 70 to 72, and 15.5° for cruises 76 and 77 (Scales, 1993). The difference between the ship's direction and its heading was then found and corrected to between 0° and 360°. The sine and cosine of the difference between the ship's head and its direction had been found, then the components of the ship's speed were calculated for each mode. The data was split into two modes, periods when the ship was port-to-wind and drifting, and periods

when it was steaming into wind. Histograms of relative wind direction were examined to determine the range of values to include in each mode. These are shown in Fig 3.3. The drifting periods were selected by choosing relative wind directions between 60° and 130° (giving a 70° 'window' on the port side) and ship's speed between 0 and 2.5 m/s. The hove to periods were selected by choosing relative wind directions between 145° and 215° , and ship's speed between 0 and 2.5 m/s. The data was then put into bins, using wind speed as the binning variable, each bin being 1 m/s wide. The mean of the components of the ship's speed, and the standard deviation of these means were calculated for each bin. At this stage the data was plotted out, and the relationship between ship's drift speed and wind speed examined.

This processing was carried out for cruises 70, 71, 72, 76 and 77 then the data was combined prior to the binning stage for each mode, and binned as a whole. The relations produced for winds on the port beam are shown in Fig 3.10, those for winds on the bow are shown in Fig 3.11.

Data Analysis and Results

Winds on the Port Beam

The data suggests:

1: There is a linear relationship between the ship's movement sideways and the wind speed, up to 17 m/s.

2: There is no significant movement in the fore/aft direction.

3: The ship's drift is non-zero in very low or no wind.

Points 1 and 2 are what we would expect. Point 3, the apparent movement of the ship in the absence of wind forcing may suggest the presence of an ocean current in the area of the ship. Admiralty charts of the North Atlantic (HD\401) state a current of 0.5 knots in a North Easterly direction over large part of the ocean in this area. This is of a similar magnitude to the drift of the O.W.S. Cumulus in low wind conditions. The charts, however, have very poor resolution so are not conclusive proof that the movement of the ship in the absence of wind is due to this current. To investigate this movement in low winds further, the data from all the cruises was selected for ship's speeds between 0 and 2.5 m/s and wind speeds of between 0 and 2 m/s. An histogram of the ship's direction of drift is shown in Fig 3.12. This clearly shows that the ship often drifts towards the North East in low winds, and is unlikely to drift in the opposite direction, towards the South West. This suggests the ship's drift in low winds is influenced by an ocean current in the vicinity of the ship. This should not be corrected for when calculating the true wind, which is defined as the wind speed relative to the sea surface.

The data between wind speeds of 7 and 17 m/s for the ship's movement sideways is shown in Fig 3.13. Cricket Graph was used to apply a linear best fit curve, forced to pass through the origin. The equation of this line is:

$$S_S = 0.0540\ U_R$$

where S_S is the ship's speed towards its starboard side, and U_R is the relative wind speed.

The histograms in Fig 3.14 show the difference between the ship's heading and its direction while drifting on a port tack. For the individual cruises, the peaks lie between 87° and 93°. The data from all five cruises is shown in Fig 3.14.a. This has a peak at 87°, but the spread of the histogram is centred around 90°. This, along with the lack of motion forwards, suggests the wind is within three degrees either side of the port beam when the ship is drifting.

Winds on the Bow

The hove to data suggests:

1: The ship's speed decreases with increasing wind speed.

2: There is a component of sideways motion while hove to.

Point 1 is what we would expect, as the direction of the wind is such that it opposes the movement of the ship. At wind speeds above 26 m/s, however, the ship is travelling backwards over the ground. The ship must make enough way through the water to keep its head into wind, so it is possible that at high wind speeds there is a wind-driven movement of the sea which carries the ship backwards at a greater speed than the ship moves through the water.

The sideways motion of the ship is of a different magnitude for each of the different cruises. Consideration of the variation in the hove to peaks given in Table 3.2 suggests that the ship heaves to with the wind at varying angles on the bow, depending on the pattern of weather during the cruise. When there is little hove to data, this suggests there were few events of heavy weather, and the average peak is at 173°. A large amount of hove to data suggests the weather was generally rough, and the probability of severe storms increases. For cruises were this is the case, the average peak is at 180°.

The greatest sideways motion is seen in the Cruise 70 data, where the sideways component is constant at 0.5 m/s for wind speeds above 12 m/s. If we consider the histogram in Fig 3.5.b, we see that the wind speed during Cruise 70 did not exceed 27 m/s, with less than 20 one-minute values for wind speed bins above 25 m/s. The Ship's Log states that the ship was hove to for one period of two days throughout the cruise. Table 3.1 shows a peak at 171°, or 9° on the port bow, for Cruise 70 from the periods when the ship was hove to. The histograms in Fig 3.15 show the difference between the ship's direction and its heading for hove to periods. Fig 3.15.b (Cruise 70 data) shows a peak at 50° which corresponds to the hove to periods. From this it can be seen that the port movement of the ship during Cruise 70 was due to the ship being held with the wind 10° on the port bow when hove to. The diagram in Fig 3.16 shows how the ship travels in this situation.

In summary, during cruises where the weather is generally rough, the ship tends to heave to with the wind directly on the bow. When there is less hove to data and the weather is generally lighter, the ship heaves to with the wind around 7° on the port bow.

The ship's movement when hove to can be related to the measured wind speed by two linear equations, one describing the ship's motion forwards, the other describing the ship's movement sideways. The forward motion relation is a linear best fit to the data from wind speeds between 12 and 30 m/s:

$$S_F = 2.06 - 0.0792\ U_R$$

where S_F is the ship's movement forwards and U_R is the relative wind speed. This is shown in Fig 3.17.

The correction for the ship's motion sideways is a constant for wind speeds between 12 and 30 m/s:

$$S_S = 0.2 \ ms^{-1}$$

where S_S is movement towards the ship's starboard side.

Comments made by the Ship's Officers

Captain Mackie and the ship's officers were shown the initial results from the analysis of data from cruises 70, 71 and 72 following Cruise 77 (Taylor, Yelland. 1993). Their comments were as follows:

They suggested the motion of the ship while drifting was with the wind either directly on or just forward of the port beam. While drifting, the ship moves through the water at up to 2 knots. The ship would heave to in winds above 17 m/s, unless there was a strong swell present, in which case the ship would heave to a lower wind speed. If the weather was coming from the south west, the ship would heave to at lower wind speeds in expectation of a heavy swell developing. When hove-to the ship is held with the wind one point (~10°) on the port bow, but in higher winds (~55 - 60 knots) the ship is pointed directly into wind. The critical speed range of the Cumulus is wide, which suggests that when hove to the engine revs are set at low level then left there. The met officers on board estimated the ship's speed through the water when hove to in relatively light winds is about 2 knots, decreasing in higher winds but always greater than half a knot. The ship travels backwards over the ground in high winds, while still making way through the water. The Master said this was due to the ship surfing backwards down swells, coupled with the effect of the wind-drift current.

Conclusions

The ship's motion as described by analysis of navigation data is confirmed by the comments of the ship's officers. The resulting linear relations will therefore provide a realistic measure of the ship's speed. The correction to apply when the ship is drifting on a port tack does not correct for the ship's movement in low winds due to a mean ocean current in the area of the ship. The equation used in the program *windcor* is:

$$S_S = 0.0540 \ U_R$$

where S_F is the ship's speed forwards and U_R is the relative wind speed. This applies for wind speeds below 17 m/s.

At high wind speeds the ship's speed over the ground is not a good approximation to the ship's speed through the water, owing to the effect of the wind-drift current. Further work is being undertaken to incorporate a value for the wind-drift current into the ship's speed correction. At this time the corrections used in the program *windcor* to apply when the ship is hove to are for the ship's speed relative to the ground:

$$S_F = 2.06 - 0.0792 \ U_R$$

and

$$Ss = 0.2\ ms^{-1}$$

where S_S is the ship's speed to starboard, S_F is the ship's speed forwards and U_R is the relative wind speed. This applies for wind speeds greater than 12 m/s.

Error Evaluation

The data from Cruise 70 was examined to evaluate the errors involved in using these relationships to calculate the ship's speed from the relative wind data. A comparison was made between the ship's speed calculated from the filtered GPS data, the ship's speed calculated using the relationships and that given by using the one-hourly position data from the Met Officers' Log, interpolated to one-minute values. Table 3.2 shows the modulus of the difference between the different methods of calculation.

The comparison between the GPS and the wind-derived speed gives a 30% lower value for the modulus of the difference than that for the GPS and the hourly position-derived speed, with 25% less error.

3.5: Propeller response correction

Young Propeller Vane

The Cumulus fast-sampled Young propeller data from Cruise 51 was processed similarly to the R.R.S. Charles Darwin data, as described in Section 2.2, and examined in the same way to determine a suitable frequency range over which to calculate the average $PSD*F^{5/3}$. The range differs for the two ships, as the propeller used on the Cumulus was a polypropylene one, heavier and more robust than the polystyrene propeller used on the Charles Darwin Cruise 43.

The differences in the Cumulus analysis are as follows:

Whereas for the Darwin the frequency range was decided by considering hove to data, for the Cumulus, the data examined was that from when the ship was drifting on a port tack (relative wind directions between 70° and 110°).

The $PSD*F^{5/3}$ flat frequency range is 0.5 to 1.2 Hz, and the distance constant calculated over this range flattens off at 2.4 m. The entire data set was corrected using this value for the distance constant, and the average $PSD*F^{5/3}$ was calculated over the range 0.5 to 1.2 Hz. The program *windcor* was used to calculate the true wind speed. The times when the ship was steaming, as stated in the Ship's Log were noted and the true wind and modus operandi variables were set absent during these periods. The pstar file is called '51avpsd', its header is shown in Fig 3.18.

The processing and analysis was repeated for Cruise 46 data, the values for the distance constant and the frequency range produced were identical to those for Cruise 51. The data was corrected using a distance constant of 2.4 m, and the average $PSD*F^{5/3}$ taken in the range 0.5 to 1.2 Hz. The true wind speed was calculated and steaming times removed. The file is called '46avpsd', and its header is shown in Fig 3.19.

Solent Sonic Anemometer

The fast sampled turbulence data collected during Cruise 70 is from the Solent sonic anemometer, so no response corrections are necessary. The average $PSD*F^{5/3}$ value for each 15-minute spectrum is calculated by the PC logging program between 2 and 4 Hz, along with the mean U, V and W wind speed and the intercept value of the spectral line (coefficient A in the pstar file). The relative wind speed and direction were calculated both from the U and V components and the U, V and W components. The program *windcors* was used to calculate the ship's speed from the U/V relative wind speed and direction, and correct the U/V/W relative wind to obtain a true wind speed. Air temperature and pressure data from the Multimet Logger was averaged onto this file using *minmid*, sea surface temperature was obtained from the Met Office Logs. The ratio of the $PSD*F^{5/3}$ value to the intercept (Coefficient A) gives a coarse value for the gradient of each spectrum, and this was used to select for clean data. The range used to define clean spectra was 0.7 to 1.3. This clean data set is called 'cleanvtrue', its header is shown in Fig 3.20.

3.6: Comparison of drag coefficient values and wave data

The data was split into periods when the ship was hove to and periods when the ship was drifting, then the program *fslcum* was used to calculate values of U10n, U*, CD and CDn. The neutral drag coefficient was then plotted against the wind speed at a measurement height of 10 metres. Cruise 46 is shown in Fig 3.21, Cruise 51 data in Fig 3.22 and Cruise 70 data in Fig 3.23. There is a discontinuity between times when the ship is drifting and when it is hove to. Where the hove to and drifting data overlap, the drag coefficient measured when the ship was drifting is higher than that measured when the ship was hove to at the same wind speed. The drag coefficient values are on average higher than the Smith (1980) relationship, the accepted value for the open ocean. The significant wave height data for Cruises 46, 51 and 70 are shown in Figs 3.24 to 3.26, plotted against wind speed at 10 metres. These scatter plots show that for a particular wind speed, the significant wave height is lower when the ship is drifting than when it is hove to. This agrees with what we know about the ship's motion, from the comments of the crew (Section 3), i.e. that the ship heaves to at a relatively low wind speed if there is a heavy swell. This suggests that the drag coefficient is higher in low wave conditions than when a large swell is present

Discussion

It is generally thought that the drag coefficient of the ocean is dependent on small, steep waves, of perhaps centimetres in height. The drag coefficient would therefore be higher than expected in young, developing seas, where the most energy is found in high frequency waves, and lower than expected in fully developed swell conditions. The data from cruises 46, 51 and 70 suggest that this may be the case.

We must, however, consider the changing orientation and speed of the ship, when hove to compared to when the ship is drifting. For each of the three cruises, the fast sampled anemometer was situated on the mid-ship goal post mast, to the port side, at a height of around 24 m above the sea surface. It is well exposed when the ship is drifting, but while hove to the ship could have a considerable effect on the turbulence in the air, and on the wind profile. The Ship Borne Wave

Recorder is unreliable a ship's speeds above 1 m/s, but it is not known whether a change in the motion of the ship from drifting sideways to hove to would significantly alter its performance.

4: R.R.S. Discovery Southern Ocean Cruise 201

4.1: Introduction

This cruise took place in early 1993 for SWINDEX (South West Indian Ocean Experiment). It was the last in a series of four Southern Ocean cruises undertaken by the R.R.S. Discovery as part of the WOCE program. The aims of SWINDEX were to observe the structure and transport of the Antarctic Circumpolar Current near the Crozet Plateau, and to deploy moorings to record time dependence of the current.

The ship departed from Cape Town on the 26th March, then made its way towards the Crozet Plateau at around 48°S 34°E. It steamed between CTD casts (typically for about six hours) and hove to at the CTD stations for about four hours. The ship returned to Cape Town on 3rd May. The cruise track is shown in Fig 4.1.

4.2: Instrumentation

The instruments deployed on the R.R.S. Discovery included a Ship Borne Wave Recorder, an em log (which records the ship's movement through the water) a bow thruster, which enabled the ship to hold its head to wind with little or no forward motion through the water when hove to, a Multimet logger taking one-minute averages of 1 Hz sampled meteorological data (air and sea temperatures, air pressure) and a fast sampled sonic anemometer giving average values for wind vectors and power spectrum density every 15 minutes.

4.3: Data Processing

The processing route used for this data set is shown in Fig 4.2. The initial file used was named mws.met.cln. This was the complete data set from the sonic anemometer after it had had the Multimet data averaged onto the fifteen minute wind spectra, then selected for relative wind directions between 120° and 240°, the scatter in the relative wind direction as a result of averaging the data to be less than 20° and the ratio of the average PSD to Coefficient A to be between 0.7 and 1.3. The true wind was found by splitting the relative wind data into along- and across-ship components, then using the em log data to correct these components for the ship's motion through the water. The components were converted to true wind speed and direction. The header of the file mws.met.cln in shown in Fig 4.3.

The program *metfluxd* was used to predict a value of U* using a relationship for the Drag Coefficient given by the data from the cruise, shown in Fig 4.4. This relation is:

$$CD \times 10^3 = 0.51 + 0.0688 U_{10}$$

where U_{10} is the wind speed at 10 metres above sea level.

The program *fsldisc* was used to calculate the measured U* and CD values from the turbulence and mean wind speed data. The difference between the measured and predicted values of U*, the U* anomaly, was found, where a positive value means that the measured friction velocity is higher than that predicted from bulk formulae. The causes of this anomaly were investigated.

4.4: Data Analysis and Results

The time derivative of the true wind speed was found using the program *pdiffr* and was compared to the U* anomaly. The data is shown in a scatter plot in Fig 4.5.a. The U* anomaly was binned on the changing wind, and this is shown in Fig 4.5.b. This shows that when the wind speed is decreasing rapidly, the measured friction velocity is higher than the bulk value. As the rate of change of wind speed goes more positive, the U* anomaly gets smaller, i.e. there is a smaller difference between the measured and predicted friction velocities.

Data from the Ship Borne Wave Recorder was examined to determine the effect of waves on the U* anomaly. The SBWR is not reliable at ship's speeds above 1 m/s, so the data above this limit was not used. A relationship between the true wind speed and the significant wave height was used to predict a wave height for any wind speed. From this a wave height anomaly was defined as the difference between the measured and predicted wave height, a positive value meaning the measured wave height is higher than the predicted height. The relation used was:

$$HsP = 3.32 - 0.136 U + 0.0181 U^2$$

where HsP is the predicted significant wave height in metres and U is the true wind speed in m/s. This is shown in Fig 4.6.

The scatter plot in Fig 4.7.a shows the wave height anomaly against U* anomaly. Fig 4.7.b shows the data in bins of U* anomaly. The data shows there is no correlation between the wave height anomaly and the U* anomaly. The plots show there is a large amount of scatter in the wave height anomaly, which suggests that relating the significant wave height at a certain time to the wind speed at the same time does not provide an accurate method of prediction. A more sensible relation would be between a time lagged wind speed and the wave measurement

A significant wind-wave height was defined in a similar way to significant wave height, but only taking the higher frequency data from the SBWR spectra. The range of frequencies used was 0.12 Hz to 0.25 Hz. The time lag which produces the optimum correlation between the wind and the waves was investigated by looking at data from jday 113 to 120. This data has relatively few gaps, the missing data points were interpolated to provide a continuous monotonic data set. The program *pcorr* calculated the optimum correlation between wind-wave height and true wind speed. Fig 4.8 shows this to occur at a 9 point or 2.25 hour lag on the wind data, i.e. the wave height is a function of the wind speed from 2.25 hours previously. The filter width to use on the wind was found by applying filters of different widths, fitting a quadratic relation to the data then comparing the correlation coefficient of the curve fit to the width of filter used. Fig 4.9 shows the optimum

filter width is 3 points, or the 45 minute mean wind speed. The relation used to predict the wind-wave height is:

$$WHsP = 1.70 - 0.0309U_{LF} + 0.00814U_{LF}^{2}$$

where WHsP is the predicted wind-wave height in metres and U_{LF} is the wind speed in m/s lagged by 2.25 hours and smoothed using a 3 point filter. This is shown in Fig 4.10.

The wind-wave height anomaly was calculated and compared to the U* anomaly. This is shown in the scatter plot in Fig 4.11.a. The data is shown binned on U* anomaly in Fig 4.11.b. Fig 4.11.b suggests there may be an inverse linear relationship between U* anomaly and wind wave height anomaly. As the U* anomaly becomes more positive, the wind wave anomaly becomes more negative.

5: Conclusions

Data from the Ocean Weather Ship Cumulus shows a possible wave effect on the Drag Coefficient. The measured Drag Coefficient is higher than the value predicted from bulk formulae during heavy swell, fully developed sea states, and lower than predicted values in developing sea conditions. The ship's effect on the measurements may be responsible for these differences, however it is possible the ship's influence increases scatter in the data, without affecting the mean measurements.

The R.R.S. Discovery SWINDEX cruise shows the measured friction velocity is higher than the predicted values during periods of sharply decreasing winds. There is a correlation between differences between the measured and predicted values of wind wave height and differences between measured and predicted values of the friction velocity. A measured wind wave height that is higher than the predicted height correlates with a friction velocity that is lower than predicted.

The data from the two ships provide contradictory results, the Cumulus data suggesting the Drag Coefficient is high in developing seas and the Discovery data suggesting a lower Drag Coefficient when the waves are higher than predicted, or if the wind speed is decreasing rapidly. The Discovery was travelling a large distance each day, and only held its position for CTD casts. This means that the ship could pass through weather systems and not see them develop, whereas the Cumulus follows the weather conditions. The two ships would have different effects on the turbulence measurements as the anemometers were in different positions. On the Cumulus the anemometer was mounted amid-ships, on the Discovery it was on the foremast.

The unknown effect of the ship's presence on measurements of the turbulence and wind field denies us conclusive evidence as to the effect of sea state on the Drag Coefficient. The Met team at the JRC have plans to quantify the ship's effect, by use of fluid dynamic modelling, and in the case of the Cumulus to request it to perform changes between drifting and hove to in a range of wind and sea states. This information will determine whether the data is erroneous due to the ship's operational status.

6: Acknowledgements

Dr P K Taylor, Margaret Yelland, Elizabeth Kent, Keith Birch, Robin Pascal.

7: References

Admiralty Chart No. 401 (Metric). *Hydrographic Office, Taunton.*

Birch, K., E. C. Kent, R. W. Pascal, P. K. Taylor, 1993: Multimet Scientific Users Guide. *James Rennell Centre Internal Document No. 10.*

Geernaert, G., 1990: The Theory and Modeling of Wind Stress with applications to Air-Sea Interaction and Remote Sensing. *Rev. Aquatic Sci.*,2, 125-149.

Hatch, M., 1993: The Ocean Weather Service. *Weather,* 48, 147-152.

Scales, M., 1993: Personal Communication. *Hydrographic Office, Taunton.*

Smith, S. D., 1980: Wind Stress and Heat Flux over the Ocean in Gale Force Winds. *J. Phys. Oceanogr.*, 10, 709-726.

Taylor, P. K., M. J. Yelland, 1993: Notes on Cumulus Visit after Cruise UK77. *Unpublished Manuscript.*

Taylor, P. K., M. J. Yelland, C. G. Davies, R. J. Tiddy, 1992: Meteorological observations on the OWS *Cumulus* - status and quality of the data set. *James Rennell Centre Internal Document No. 6.*

Taylor, P. K., M. H. Smith, W. J. Gould, 1991: RRS Charles Darwin Cruise 43. *Institute of Oceanographic Sciences Deacon Laboratory Cruise Report* No 227.

Ward, S. K., R. W. Pascal and K. G. Birch, 1993: *Meteorological data from RRS Charles Darwin Cruise 73.* Internal Document 12, James Rennell Centre, Southampton, UK, pp. 16.

Yelland, M. J., P. K. Taylor, I. E. Consterdine, M. H. Smith, 1993: The Use of the Inertial Dissipation Techinique for Shipboard Wind Stress Determination. *(Submitted to J.Atmos.Ocean. Technology)*

8: Tables

Cruise Number	Hove to relative wind direction/°	Port Drift relative wind direction/°	Proportion of cruise hove to	Instrument
44	169	71	Large	Young
45	161	69	Small	Young
46	167	69	Small	Young
50	165	71	Medium	Young
51	156	70	Large	Young
52	152	69	Small	Young
54	155	73	Small	Young
55	-	69	None	Young
56	-	67	None	Young
57	-	61	None	Young
Mean of Small	159		Small	Young
Mean of Large	163		Large	Young
Mean of All		69		Young

Table 3.1: Data from histograms of relative wind direction for cruises when the Young vane was deployed. The peaks in the histograms relating to hove to and drifting are shown for each cruise.

Cruise Number	Hove to relative wind direction/°	Port Drift relative wind direction/°	Proportion of cruise hove to	Instrument
70	171	93	Small	Solent Sonic
71	177	92	Large	Solent Sonic
72	183	93	Large	Solent Sonic
76	175	95	Small	Solent Sonic
77	-	93	None	Solent Sonic
Mean of Small	173		Small	Solent Sonic
Mean of Large	180		Large	Solent Sonic
Mean of All		93		Solent Sonic

Table 3.2: Data from histograms of relative wind direction from cruises carrying the Solent sonic anemometer. The peaks in the histograms relating to hove to and drifting are shown for each cruise.

	Cruise 71 Data		
	Port Winds	Bow Winds	All Data
|GPS - Met| (m/s)	0.2±0.22	0.2±0.19	0.21±0.25
|GPS - WDS| (m/s)	0.15±0.17	0.2±0.17	0.17±0.18
|WDS - Met| (m/s)	-	-	0.22±0.19

Table 3.3: Evaluation of the errors in ship's speed arising from the different methods of calculation. GPS indicates the ship's speed calculated from the filtered one-minute GPS data, Met indicates the ship's speed calculated from the one-hourly positions in the Met Log interpolated to one-minute values, and WDS indicates the ship's speed calculated from the linear ship's speed/wind speed relationships.

9: Figures

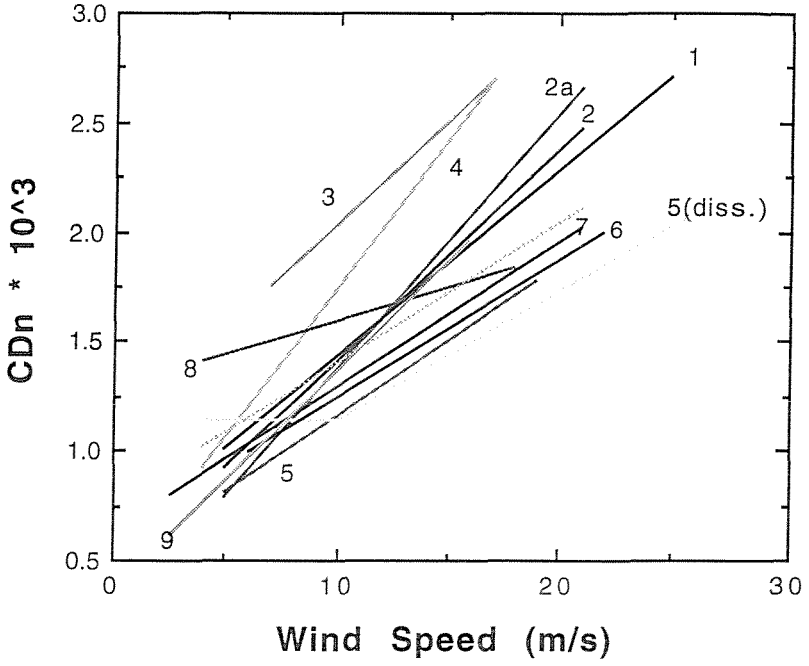

Figure 1.1: Summary of recent studies of the Drag Coefficient made by Geernaert (1990). The graph shows Neutral Drag Coefficient plotted against wind speed at 10 metres.

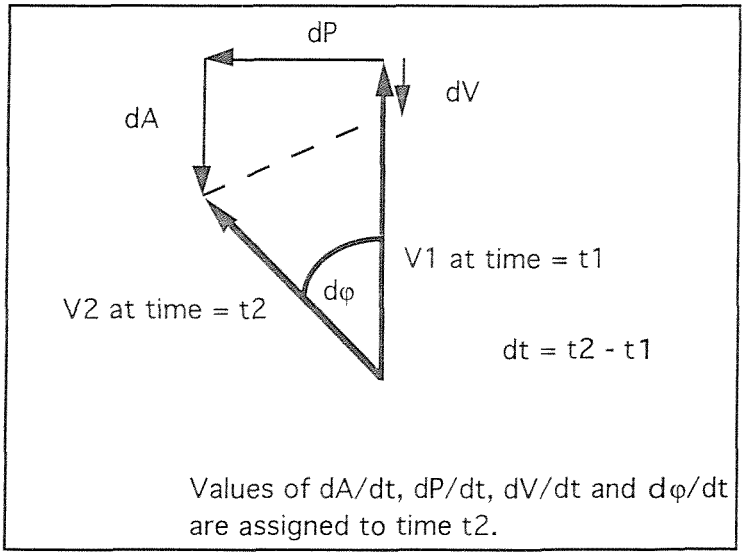

Figure 1.2: Method of calculation of the changing wind vector performed by the subroutine *deltasub* in the pstar program *deltawind*.

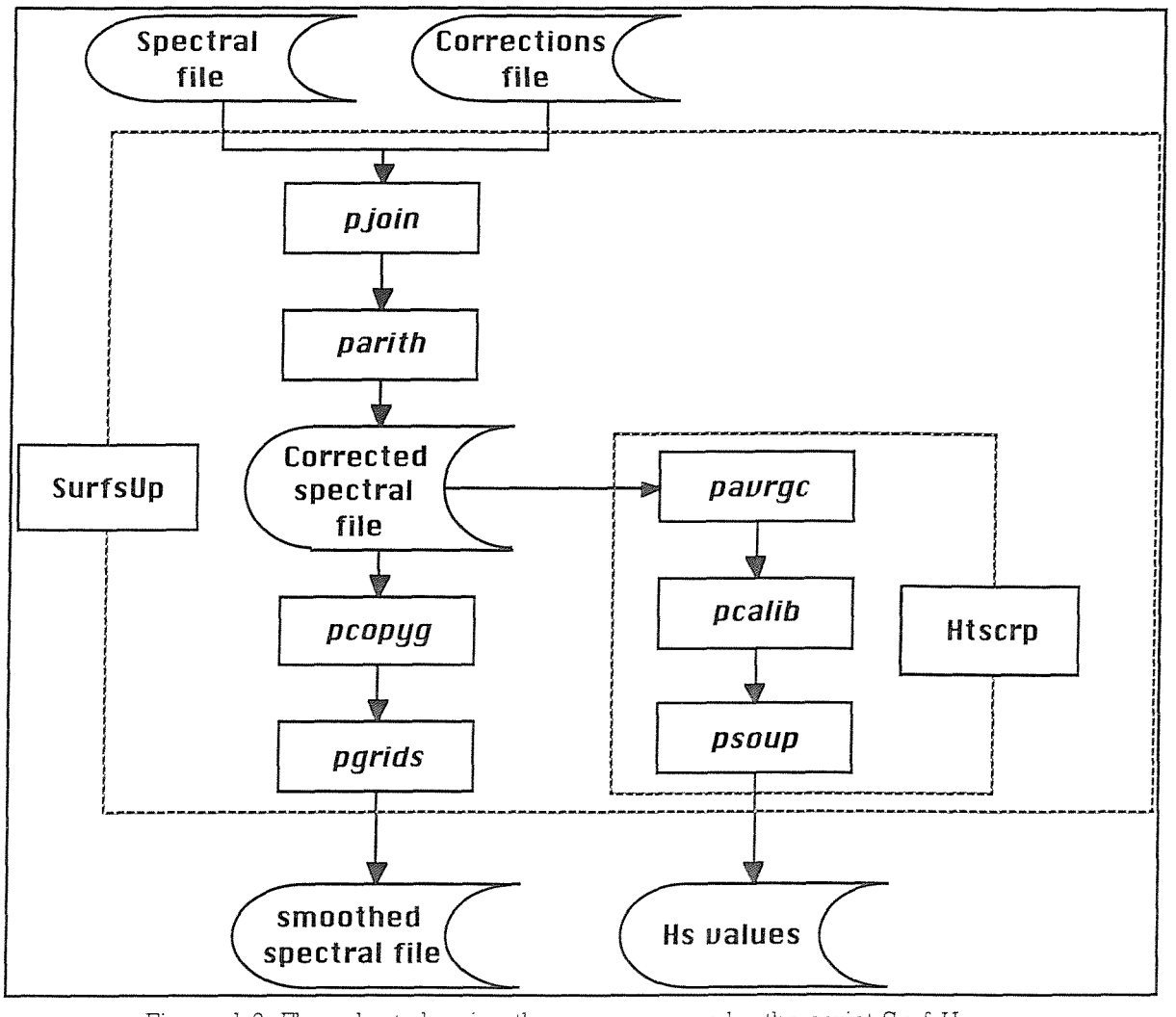

Figure 1.3: Flow chart showing the programs run by the script SurfsUp.

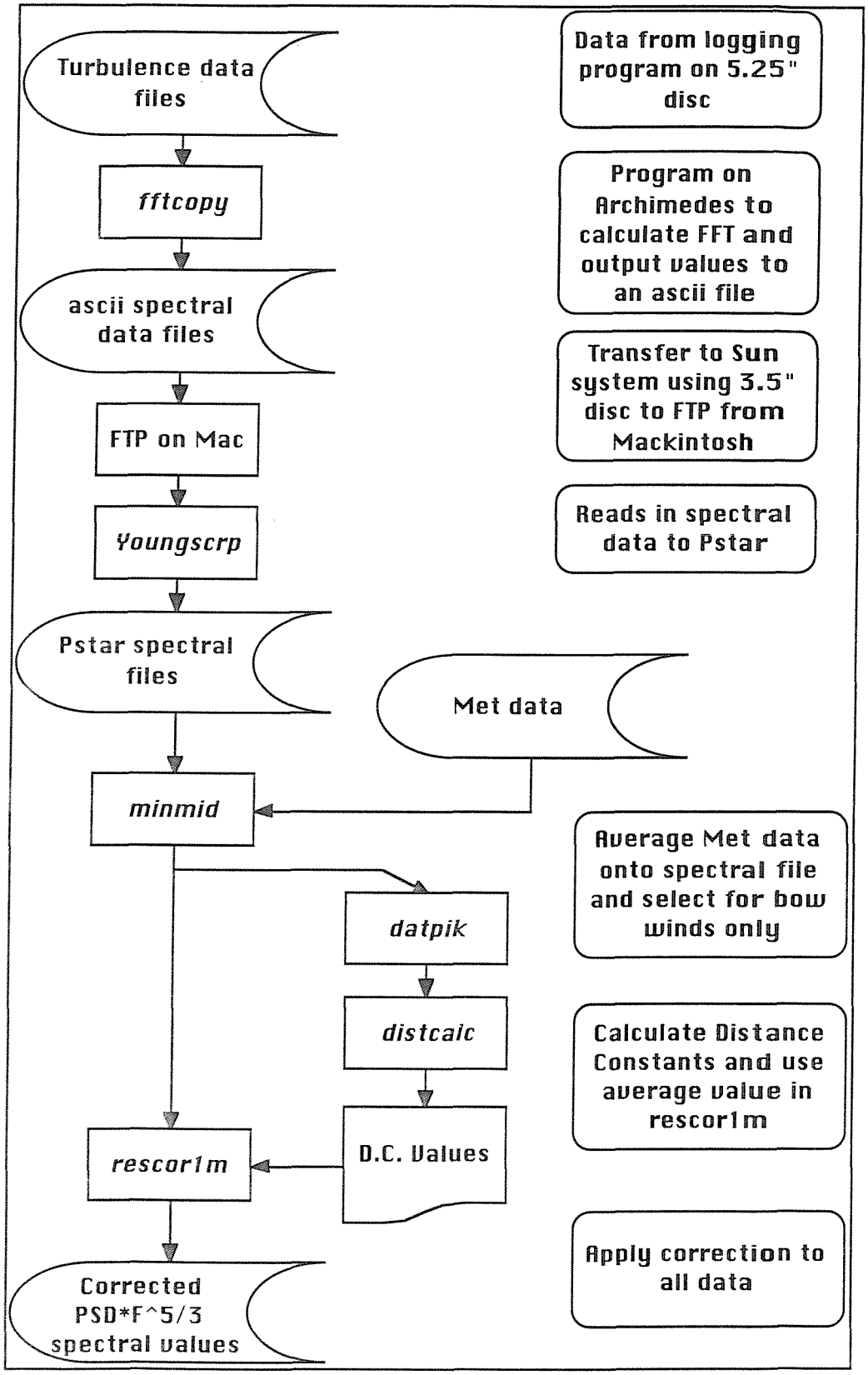

Figure 2.1: Flow chart showing the processing route for Young Propeller Vane turbulence data.

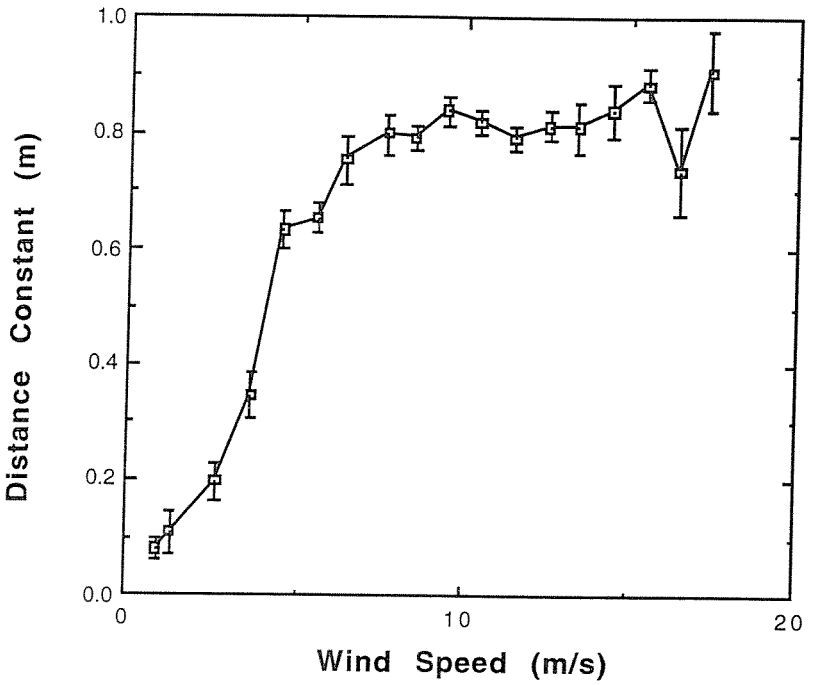

Figure 2.2: Distance Constant calculated between 1 and 2 Hz against wind speed.

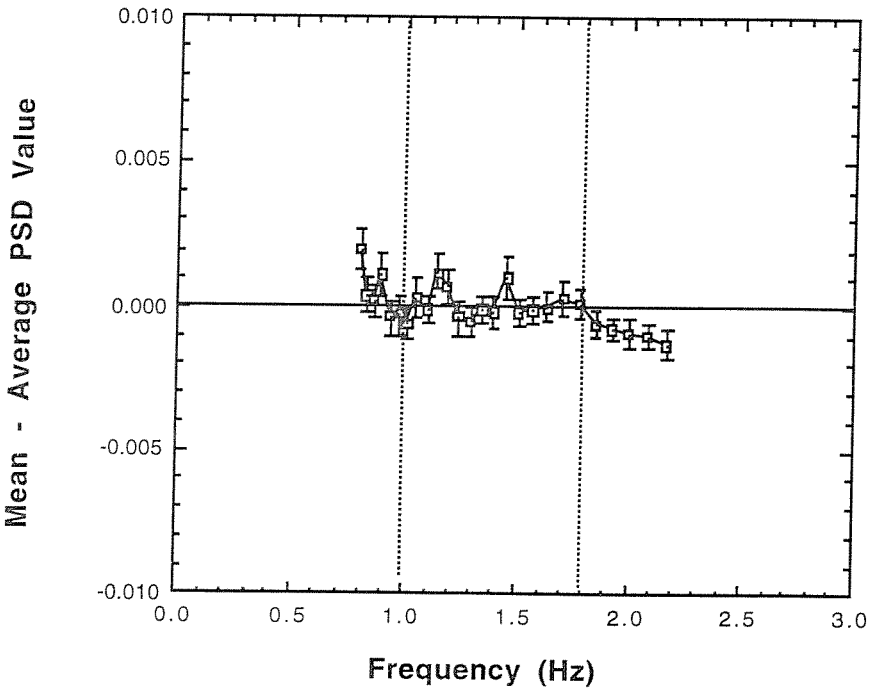

Figure 2.3: Normalised PSD*$F^{5/3}$ against frequency. The dashed lines show the range in which the spectra are flat.

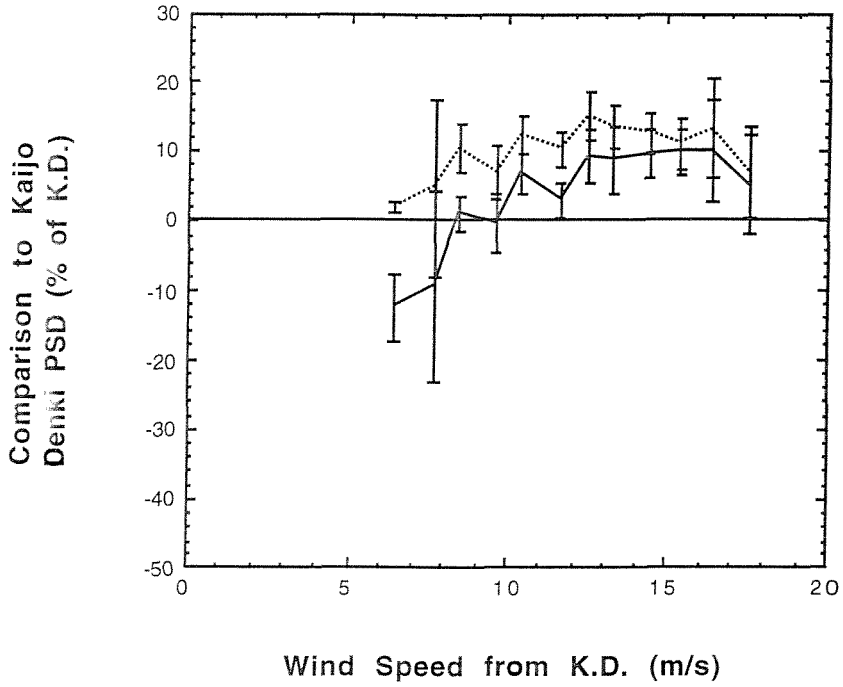

Figure 2.4: Comparison between PSD values from the Young and the Kaijo Denki anemometers against wind speed, shown as a percentage of the Kaijo Denki value.

```
DATA DESCRIPTION
****************                    ****************          Prefil:
                          Data Name: *Young      ruZD*          Postfl:
                                     ****************
Even samp:
Archive flag:                            Platform                Depth of   Depth of
Raw data flag: P              **Type** ****Name**** *Number*   instrument   water
Instrument:MultiMet           ship     darwin       cr 43          0.00M      0.00M

Fields (Vars):  23    Data cycles:    113    (2/3D: NROWS:   0   NPLANE:   0)
Start time: 0/     0/000000  Position:  0.0000   0.0000( 0  0.00N   0  0.00E)
*********************************************************************************
*   Field    * Units  *   Lower Limit   *   Upper Limit   * Absent data val *
*********************************************************************************
*  1.JDAY    *DAYOFYR *         308.628 *         323.161 *         -999.000 *
*  2.PSD NE.M*        *           0.005 *           0.213 *         -999.000 *
*  3.vvyg  .M*M/S     *           4.285 *          17.866 *         -999.000 *
*  4.PSDF C.M*        *           0.004 *           0.254 *         -999.000 *
*  5.U CORR.M*M/S     *           4.522 *          17.720 *         -999.000 *
*  6.k-s psd%*        *         -26.595 *          19.003 *         -999.000 *
*  7.k-y psd%*        *         -32.593 *          32.256 *         -999.000 *
*  8.y-s psd%*        *         -36.921 *          26.836 *         -999.000 *
*  9.k-s u%k *        *          -8.753 *           4.672 *         -999.000 *
* 10.k-y u%k *        *          -5.762 *          11.672 *         -999.000 *
* 11.y-s u%k *        *         -17.607 *           5.184 *         -999.000 *
* 12.DIRN  .M*DEGREES *         160.029 *         189.269 *         -999.000 *
* 13.DIRN  .S*DEGREES *           1.581 *           9.916 *         -999.000 *
* 14.jday  .M*days    *         308.631 *         323.162 *         -999.000 *
* 15.jday  .S*days    *           0.000 *           0.000 *         -999.000 *
* 16.Freq  .M*Hz      *           1.362 *           1.362 *         -999.000 *
* 17.Freq  .S*Hz      *           0.000 *           0.000 *         -999.000 *
* 18.vvyg  .M*M/S     *           4.289 *          17.841 *         -999.000 *
* 19.vvyg  .S*M/S     *           0.000 *           0.000 *         -999.000 *
* 20.Sf5/3 .M*        *           0.004 *           0.211 *         -999.000 *
* 21.Sf5/3 .S*        *           0.000 *           0.000 *         -999.000 *
* 22.k-y.81  *        *          -0.024 *           0.060 *         -999.000 *
* 23.k-yg.81 *%k-d    *         -18.891 *          38.505 *         -999.000 *
*********************************************************************************
```

Figure 2.5: Pstar header for the file 'cd43anemoms' where 'PSD NE.M' is the original Young PSD, 'PSDF C.M' is the Kaijo Denki PSD and 'Sf5/3 .M' is the reprocessed Young data.

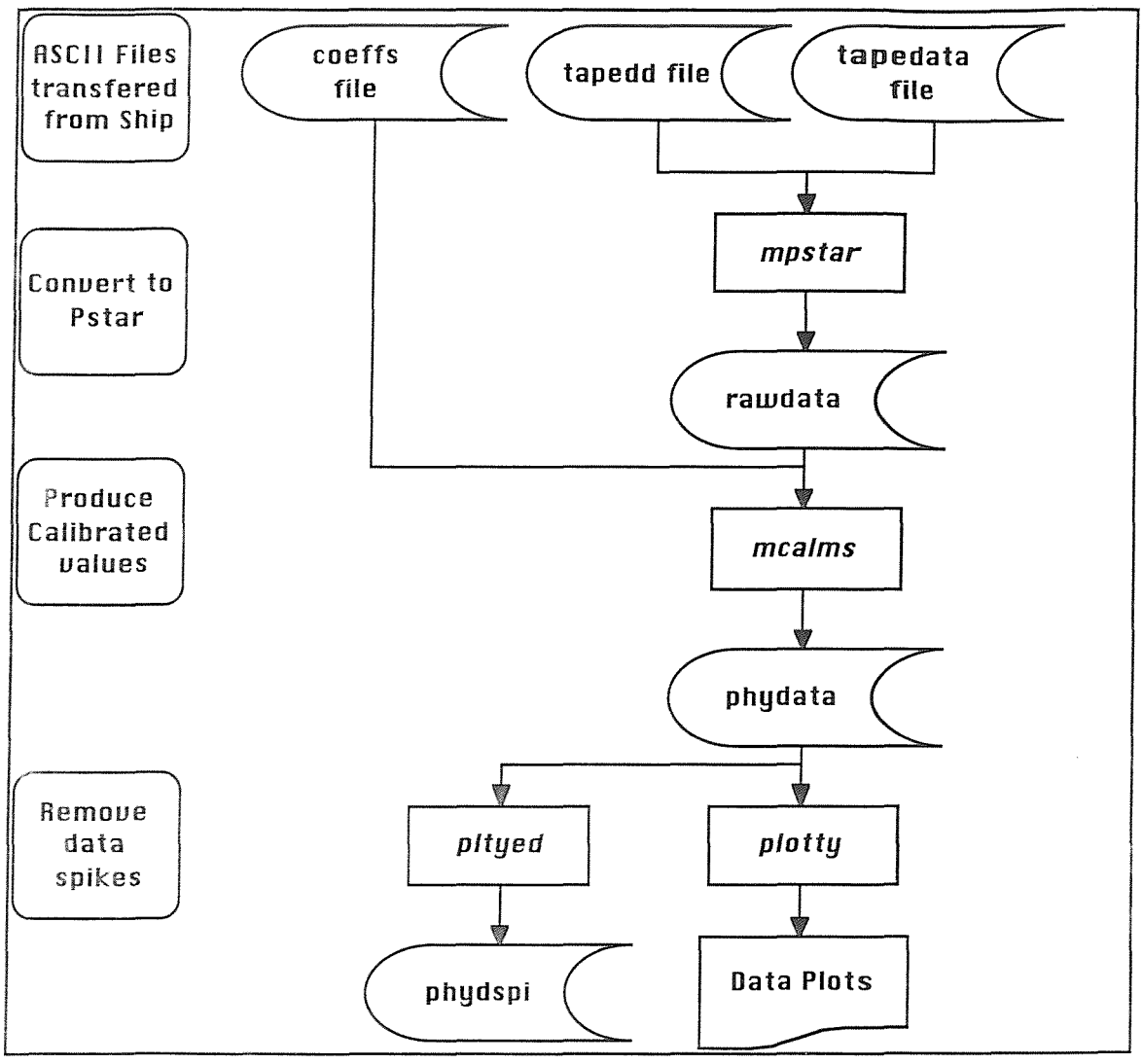

Figure 3.1: Processing route for the Cumulus slow sampled data from the Multimet Logger.

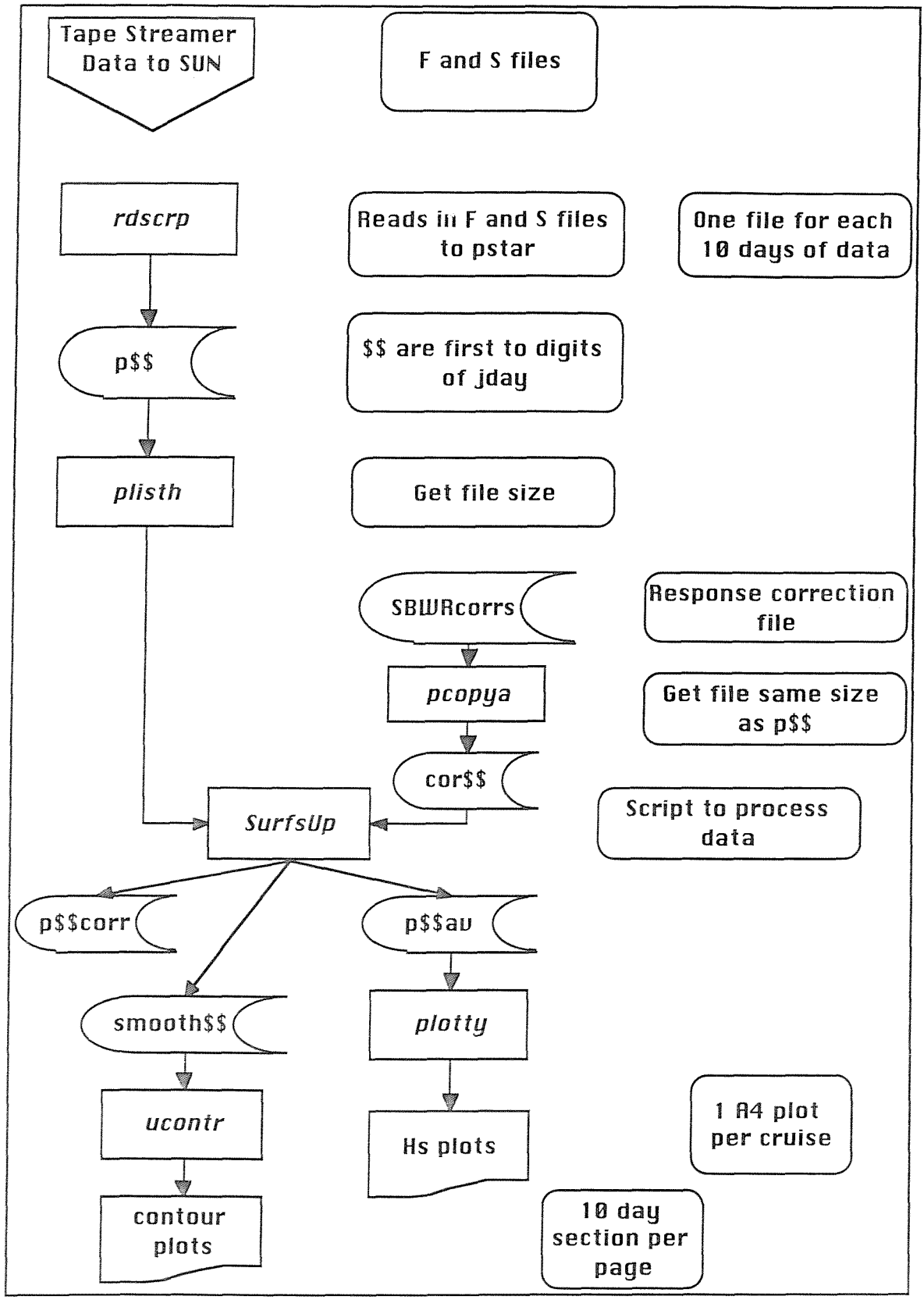

Figure 3.2: Processing route for Ship Borne Wave Recorder data.

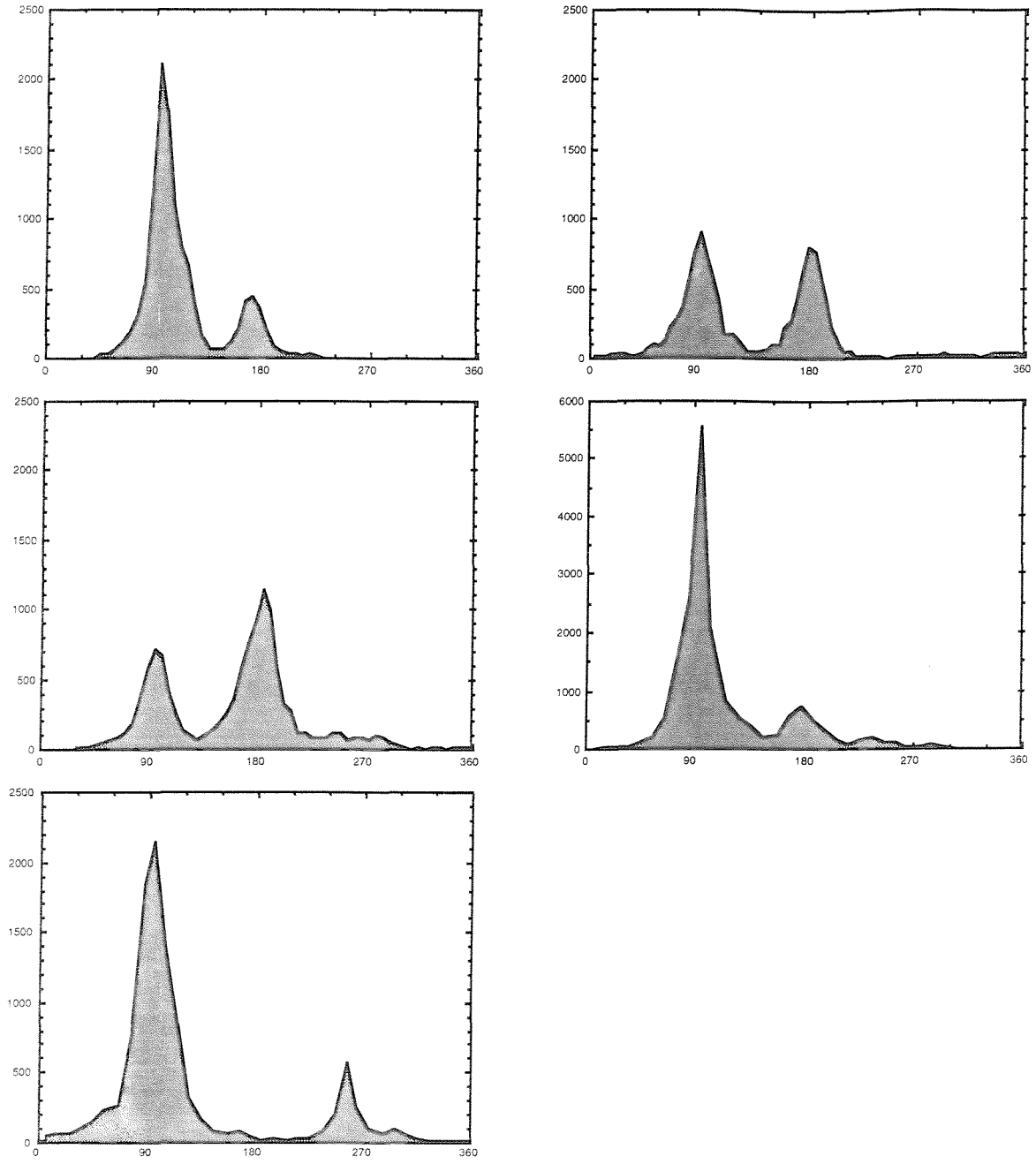

Figure 3.3: Histograms of relative wind direction from cruises carrying the Solent Sonic anemometer. Fig a) shows data from Cruise 70, b) shows Cruise 71 data, c) shows Cruise 72 data, d) shows Cruise 76 data and e) shows data form Cruise 77. The bin width is 10°.

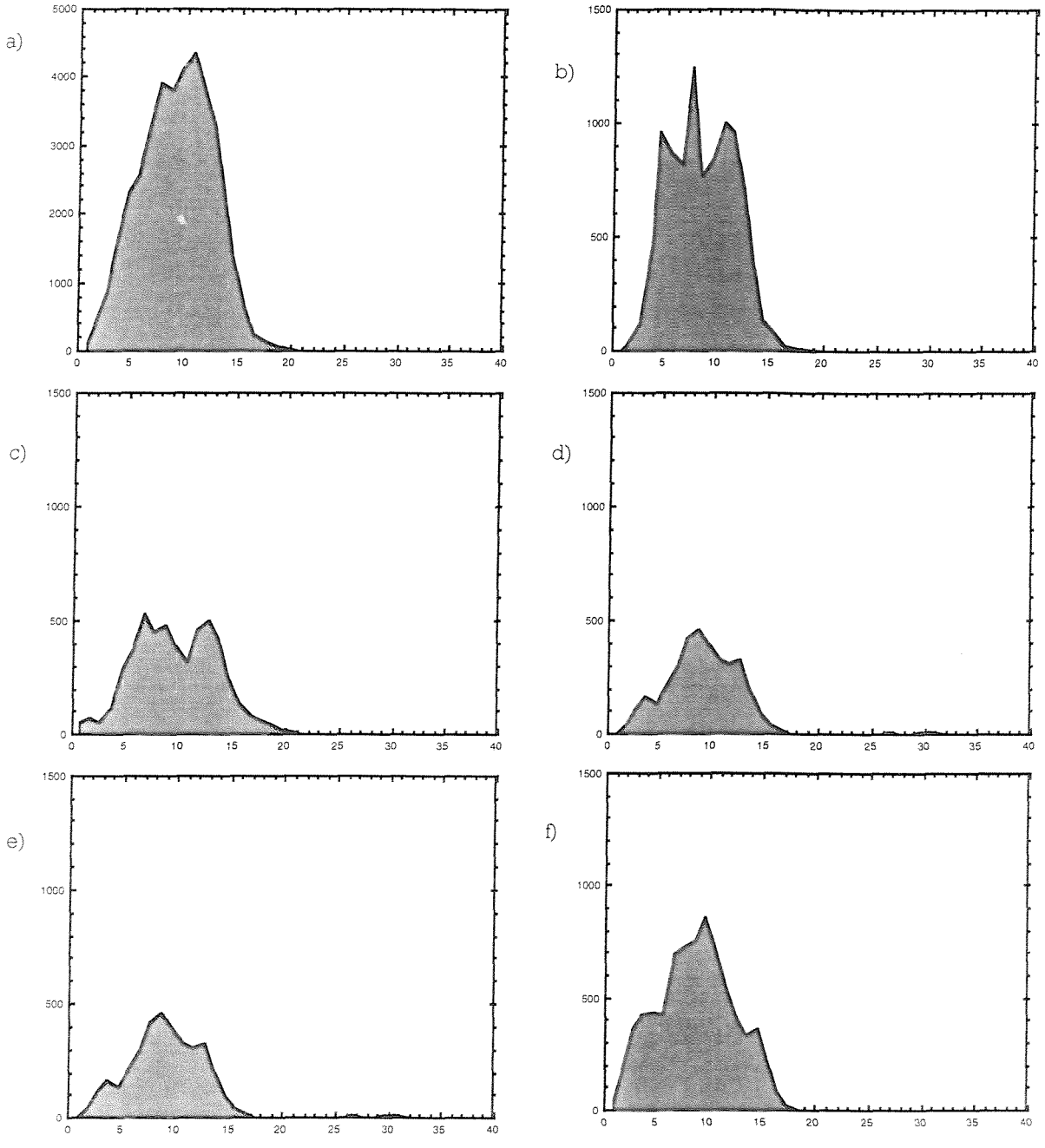

Figure 3.4: Histograms of one-minute observations taken at each wind speed when the ship was drifting. Fig a) shows data from all 5 cruises, Figs b) to f) show data from cruises 70, 71, 72, 76 and 77 respectively. The bin width is 1 m/s.

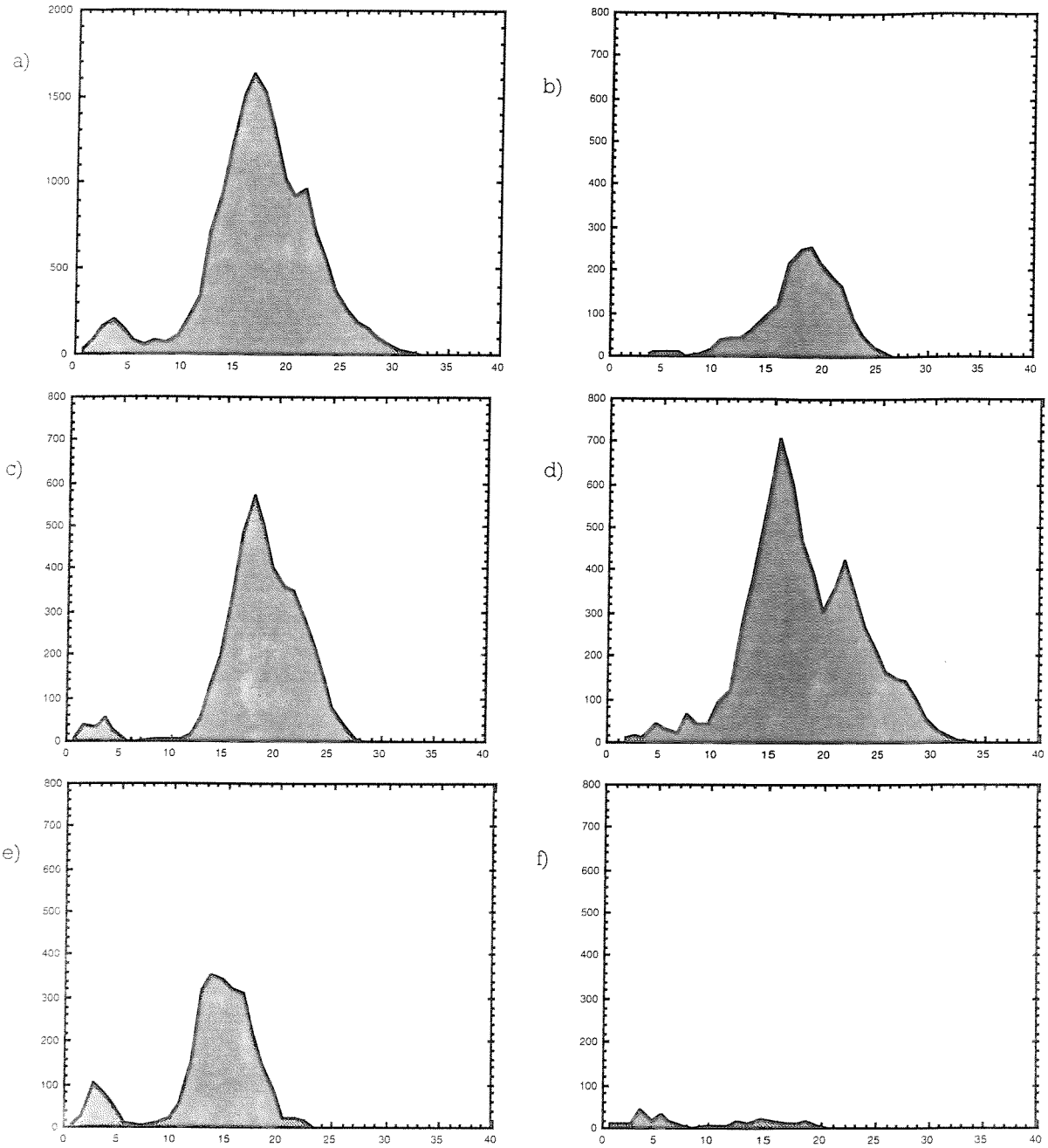

Figure 3.5: As Fig 3.4 but for times when the ship was hove to.

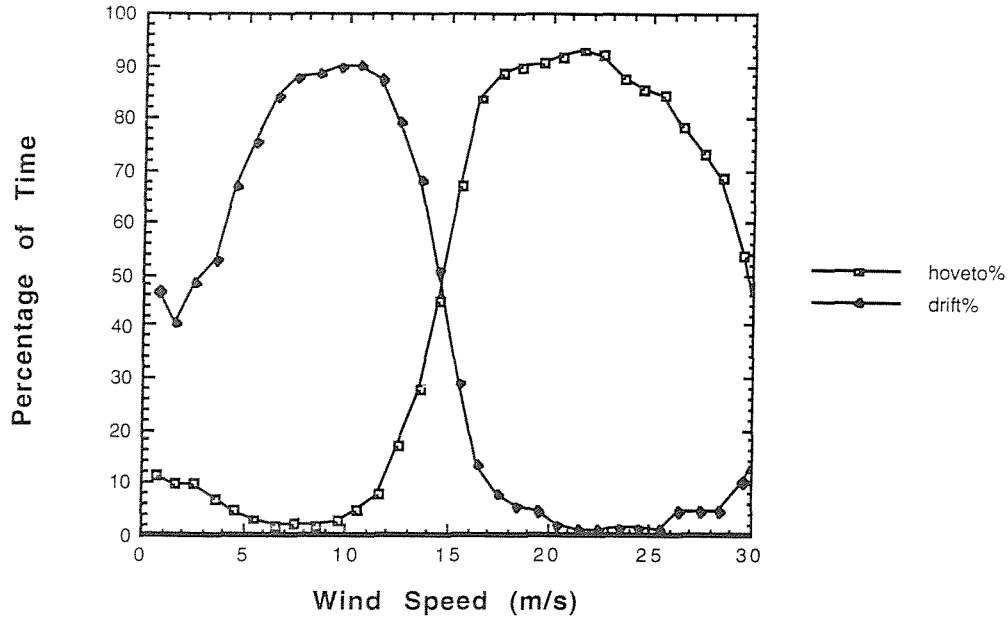

Figure 3.6: Percentage of time the ship spends drifting and hove to as a function of wind speed.

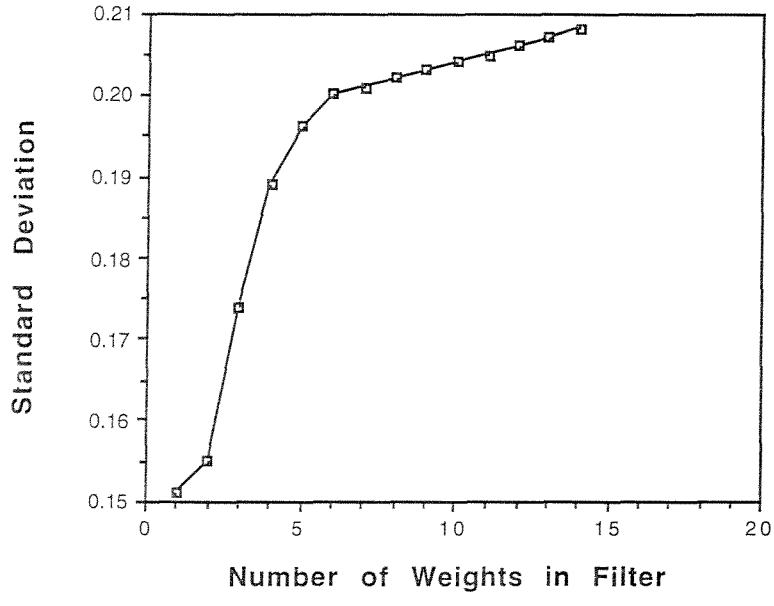

Figure 3.7: Standard deviation of the mean difference between speed calculated from raw position data and that calculated from filtered position data against the number of weights used in the filter.

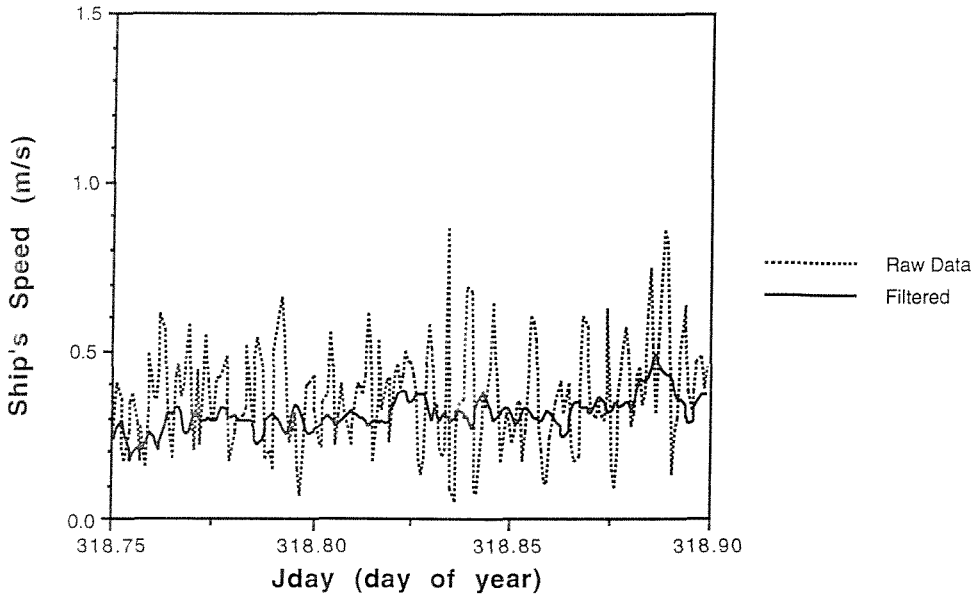

Figure 3.8: A comparison of speed calculated from raw position data and speed calculated from the same data after the optimum filter has been applied.

Figure 3.9 (over page): Processing route used for Cumulus data in examining the relationship between the ship's speed and the wind speed. The names of the Pstar programs are shown in italics.

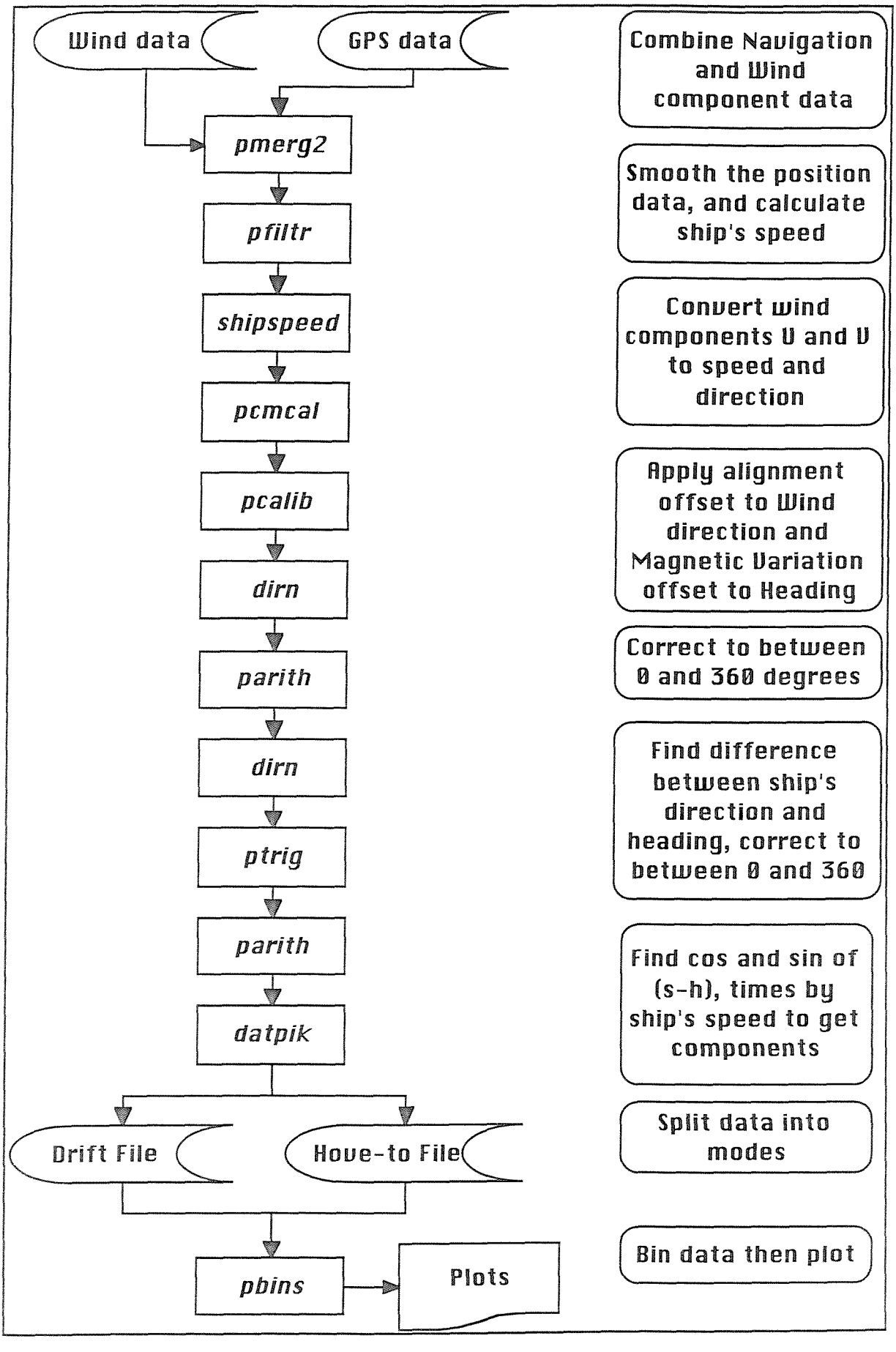
Wind data
GPS data
Combine Navigation and Wind component data
pmerg2
pfiltr
Smooth the position data, and calculate ship's speed
shipspeed
Convert wind components U and V to speed and direction
pcmcal
pcalib
Apply alignment offset to Wind direction and Magnetic Variation offset to Heading
dirn
parith
Correct to between 0 and 360 degrees
dirn
ptrig
Find difference between ship's direction and heading, correct to between 0 and 360
parith
datpik
Find cos and sin of (s-h), times by ship's speed to get components
Drift File
Hove-to File
Split data into modes
pbins
Plots
Bin data then plot

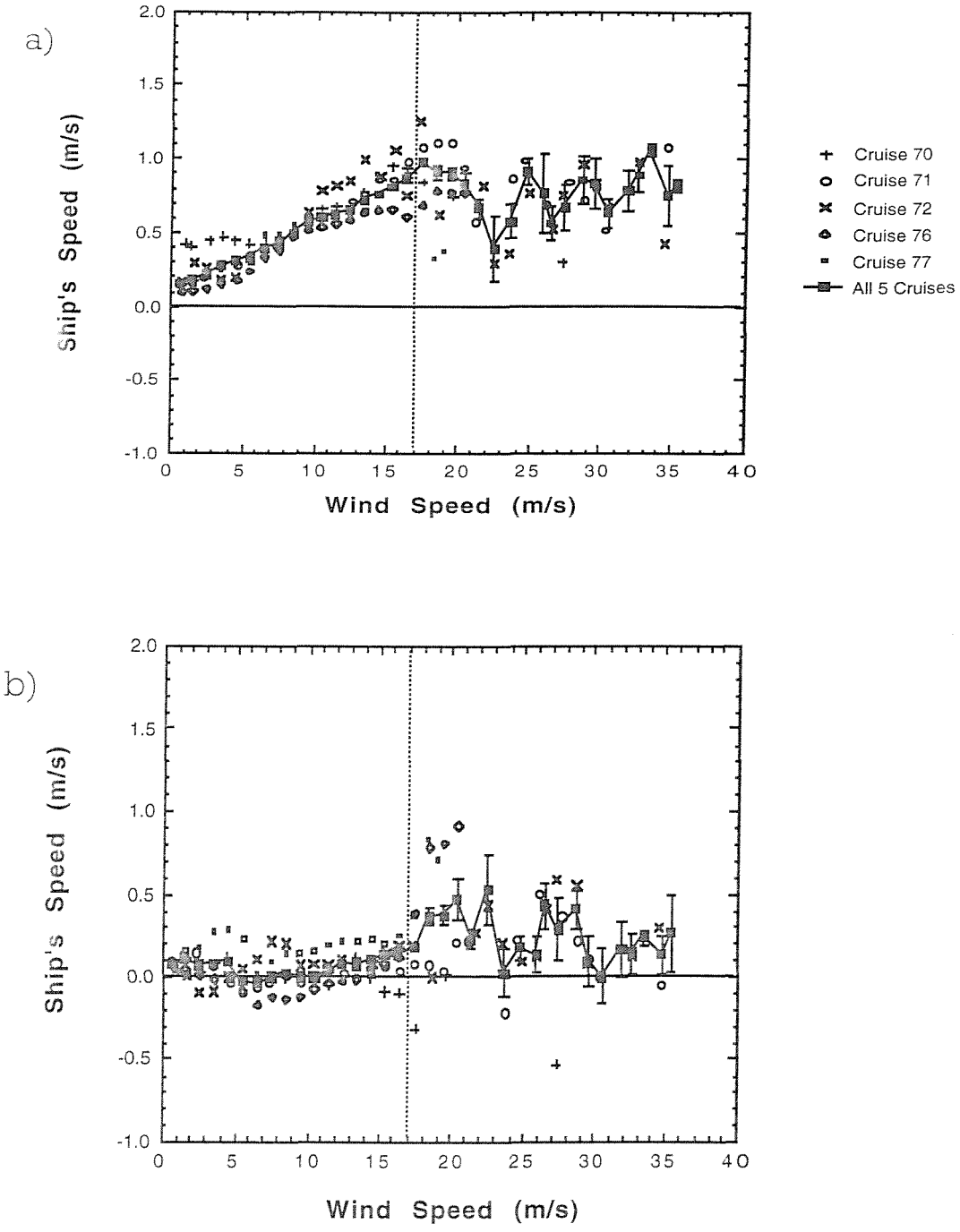

Figure 3.10: Ship's speed against wind speed. Fig a) shows the ship's motion sideways (towards starboard being positive), Fig b) shows the ship's motion forwards. The dashed line shows the upper limit above which there is very little data.

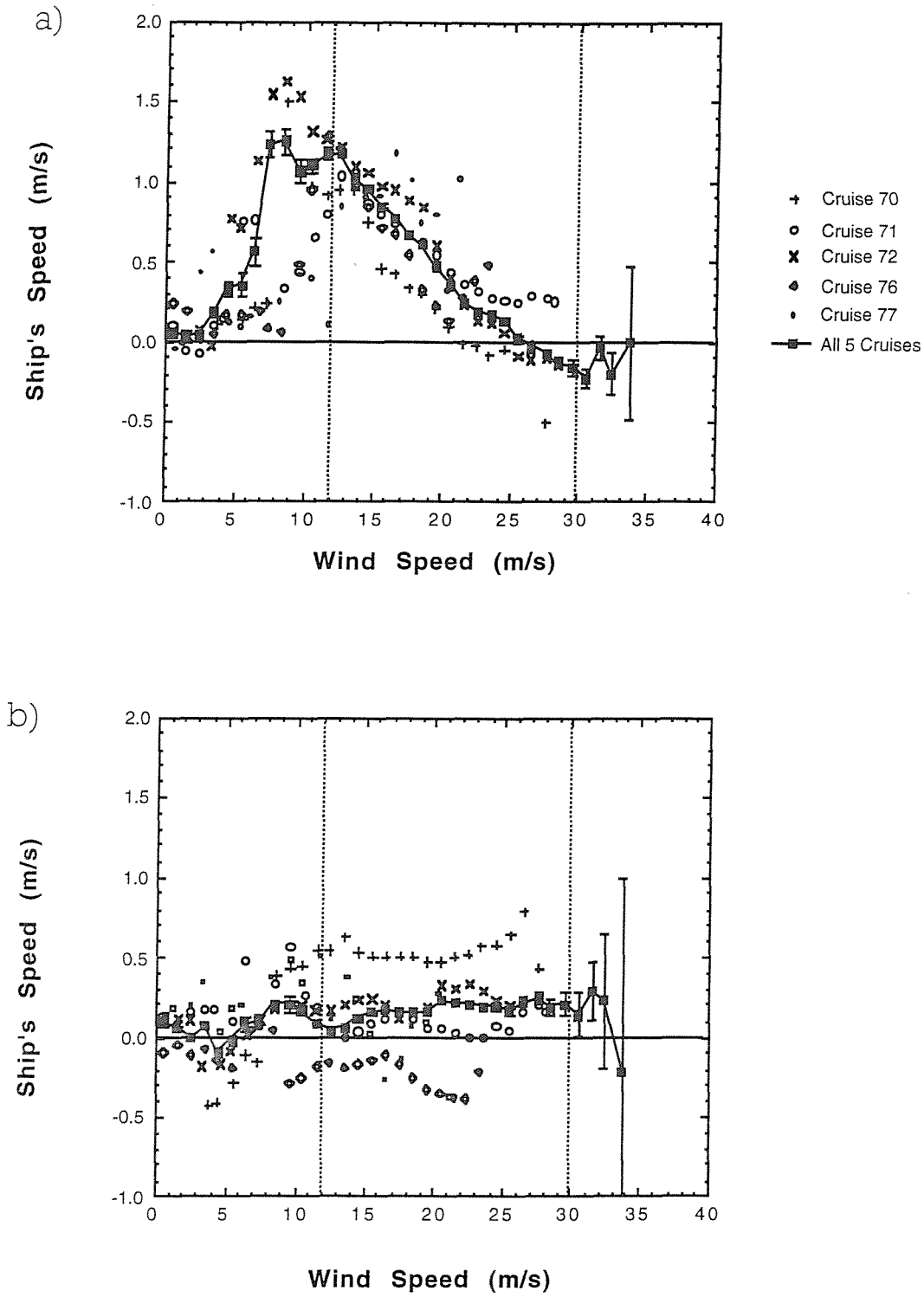

Figure 3.11: Ship's speed against wind speed. Fig a) shows the ship's motion forwards, Fig b) shows the ship's motion towards starboard. The dashed lines show the range outside of which there is very little data.

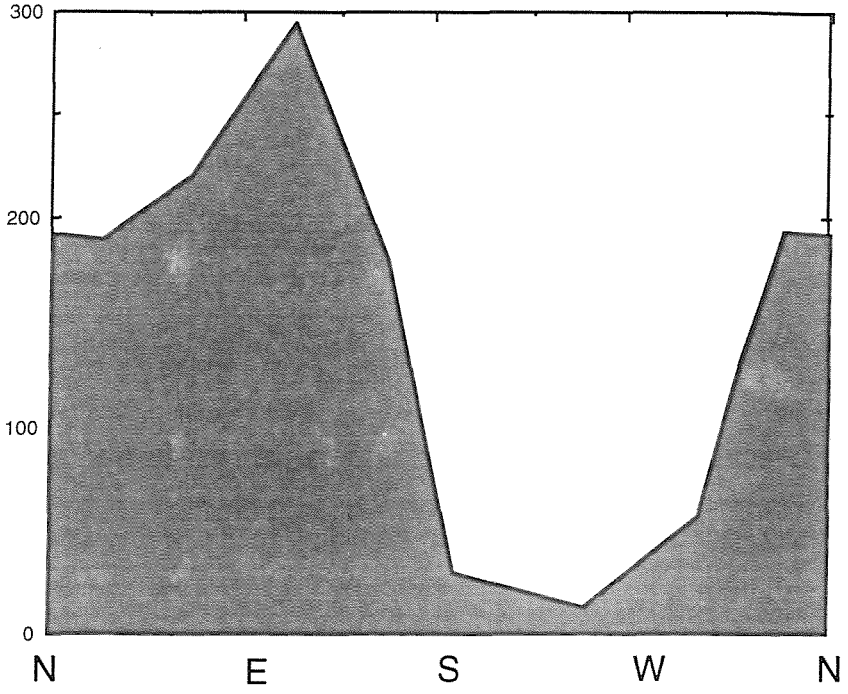

Figure 3.12: Histogram of ship's direction of travel in wind speeds less than 2 m/s. The bin width is 45°.

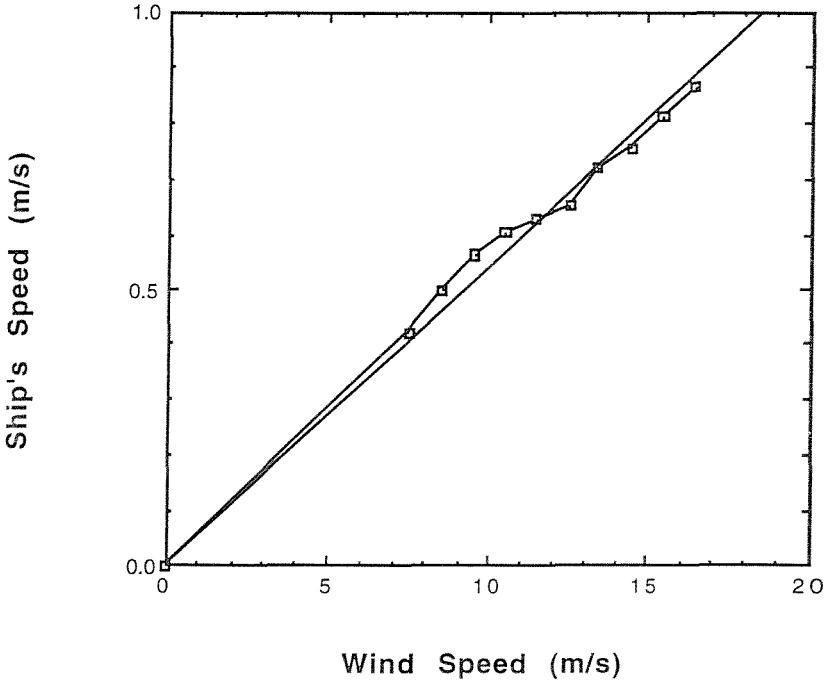

Figure 3.13: Ship's speed sideways (towards starboard positive) against wind speed for winds between 7 and 17 m/s and on the port beam. The equation of the line of best fit is S = 0.0540 U.

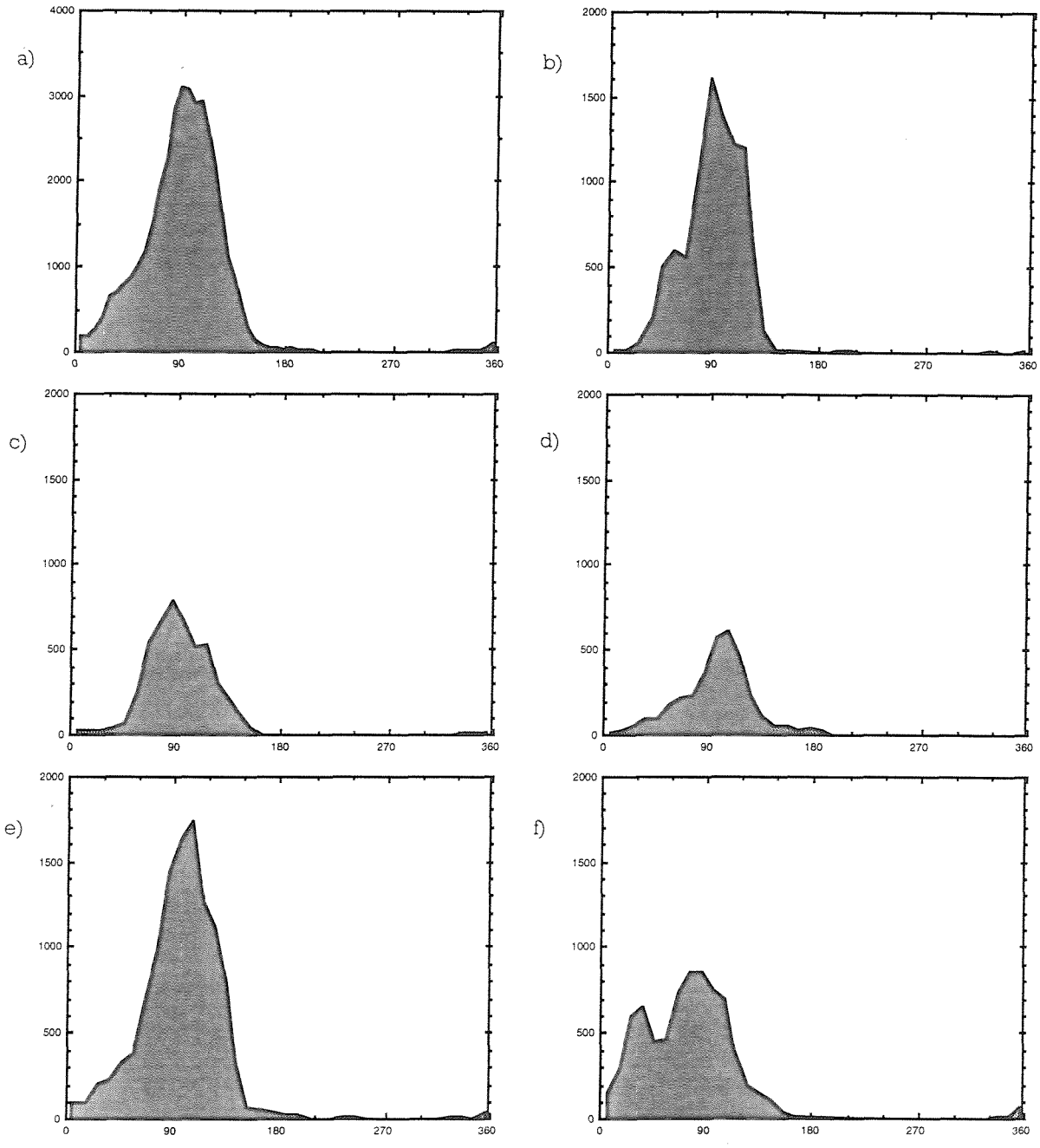

Figure 3.14: Histograms of the difference between the ship's heading (the direction the ship is pointed) and its direction of travel while drifting. Fig a) shows data from all 5 cruises, b) to f) show data from cruises 70, 71, 72, 76 and 77 respectively. The bin width is 10°.

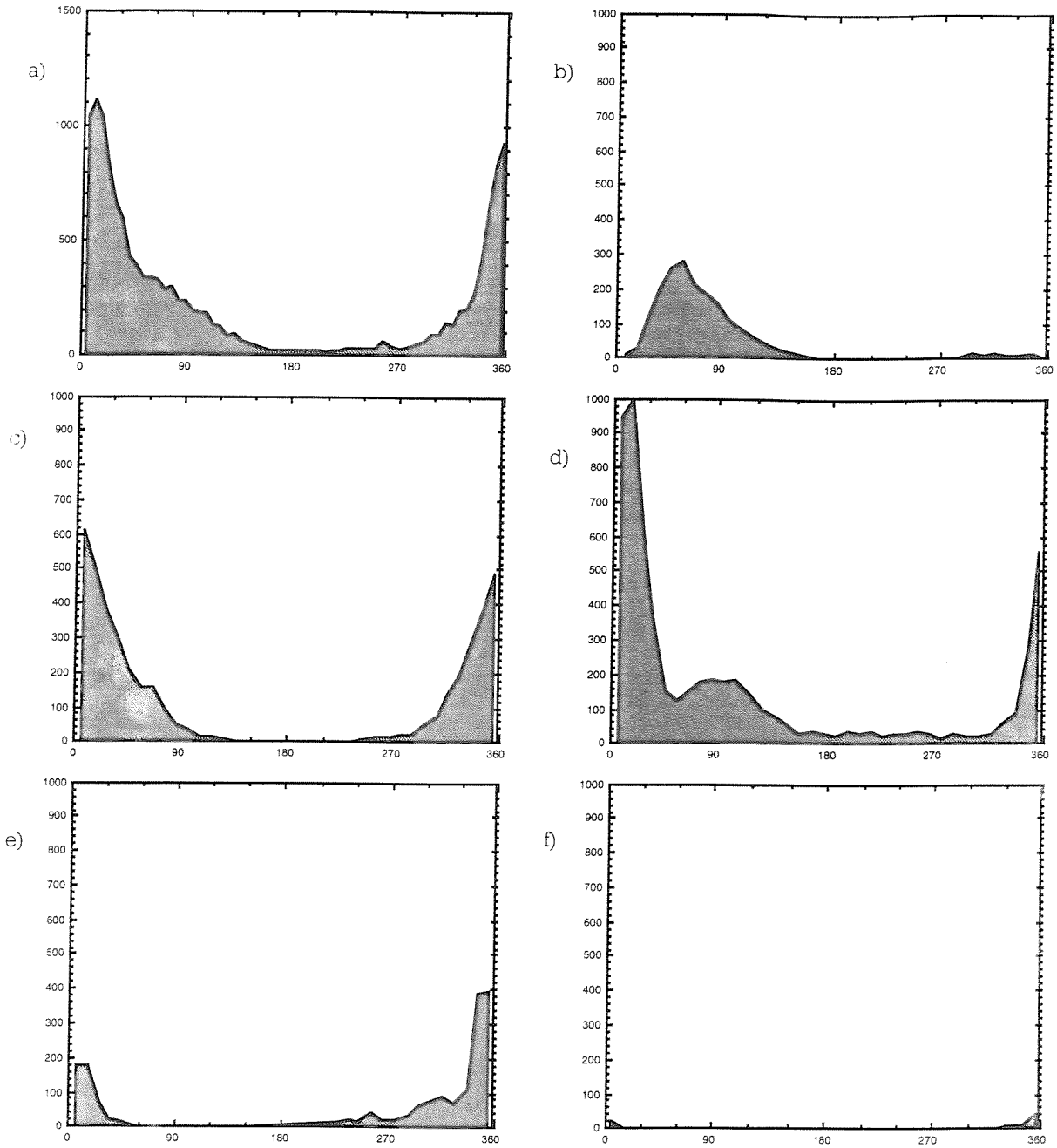

Figure 3.15: As Fig 3.14 except for times when the ship is hove to.

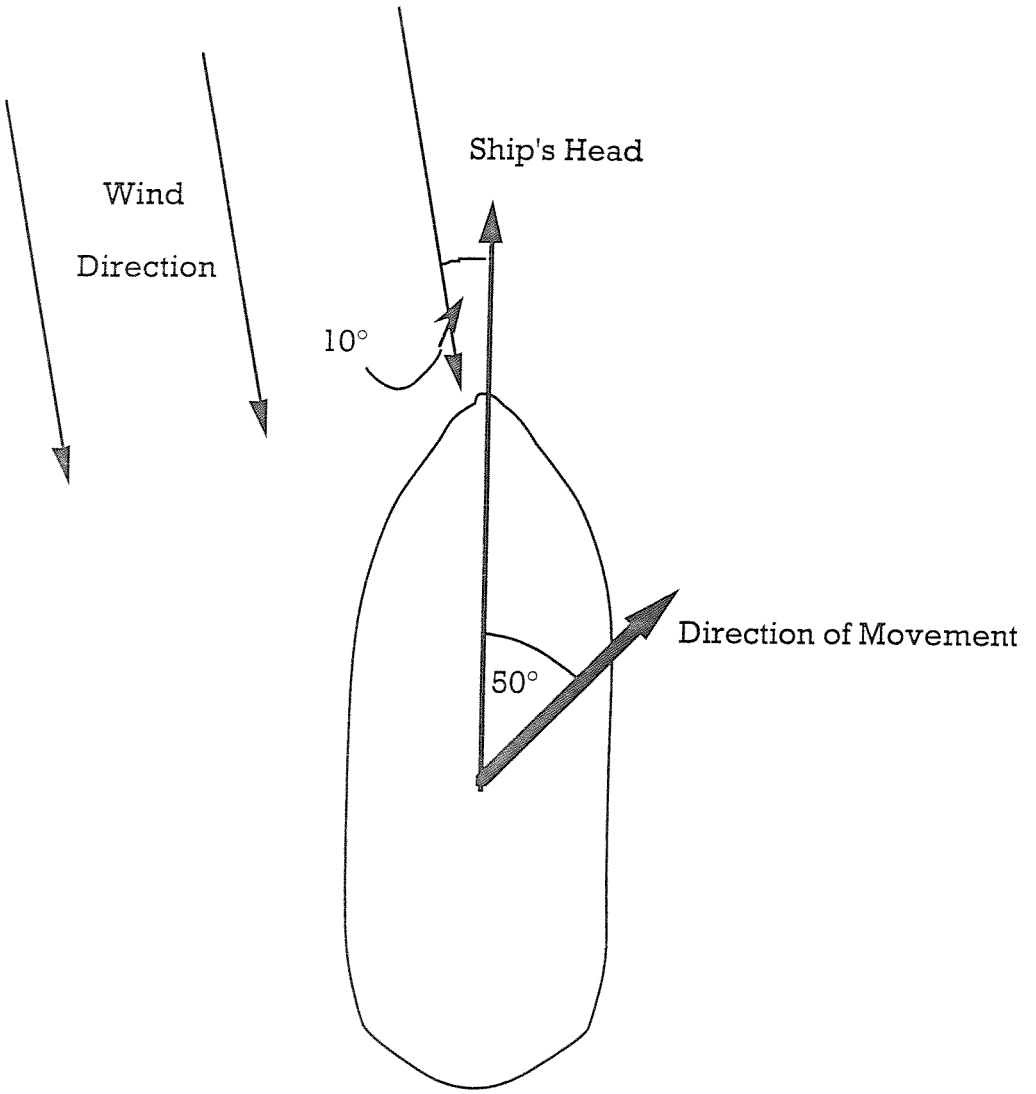

Figure 3.16: The ship's motion when hove to as described by data from Cruise 70.

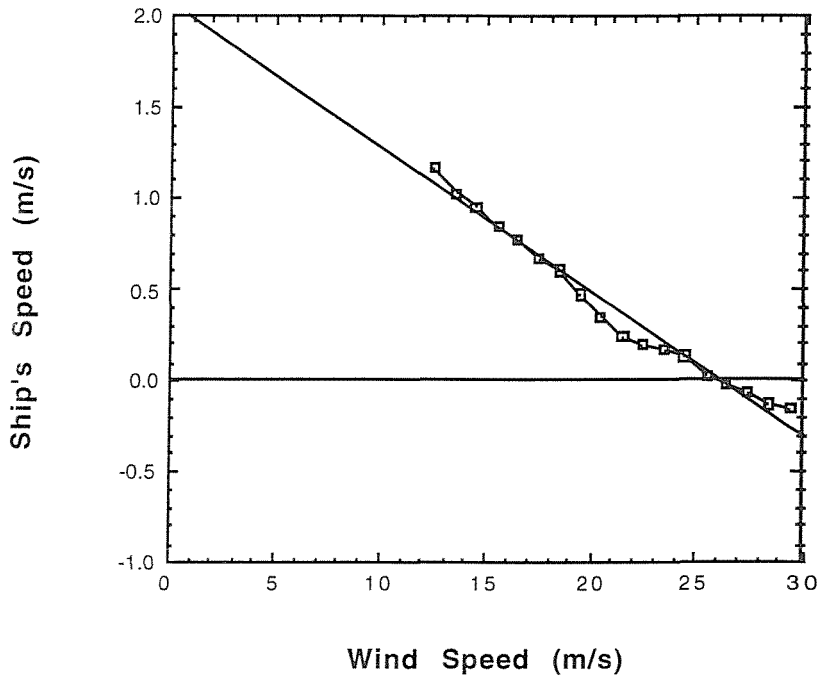

Figure 3.17: Ship's speed forwards against wind speed for winds between 12 and 30 m/s and on the bow. The equation of the line of best fit is S = 2.06 - 0.0792 U.

```
DATA DESCRIPTION
****************                    ****************          Prefil:
                          Data Name: *Young      ruER*          Postfl:
                                     ****************

Even samp:
Archive flag:                            Platform              Depth of  Depth of
Raw data flag: P                 **Type** ****Name**** *Number*  instrument  water
Instrument:various               Ship     Cumulus      Cum46        0.00M     0.00M

Fields (Vars):  21    Data cycles:   2681    (2/3D: NROWS:   0   NPLANE:   0)
Start time: 0/     0/000000  Position:  0.0000   0.0000( 0  0.00N   0  0.00E)
*********************************************************************************
*   Field    * Units  *   Lower Limit   *   Upper Limit   * Absent data val *
*********************************************************************************
*  1.jday    *days    *         150.470 *         183.077 *        -999.000 *
*  2.Freq    *Hz      *           0.823 *           0.823 *        -999.000 *
*  3.log10PSD*        *          -6.463 *          -2.473 *        -999.000 *
*  4.VVyng .M*m/s     *           0.150 *          24.250 *        -999.000 *
*  5.VVyng .S*m/s     *           0.000 *           3.282 *        -999.000 *
*  6.DDyng .M*degrees *          19.191 *         336.774 *        -999.000 *
*  7.DDyng .S*degrees *           0.000 *         141.797 *        -999.000 *
*  8.PRESS .M*mb      *         987.137 *        1026.009 *        -999.000 *
*  9.PRESS .S*mb      *           0.000 *           0.421 *        -999.000 *
* 10.TWport.M*degc    *           5.190 *          11.703 *        -999.000 *
* 11.TWport.S*degc    *           0.000 *           0.411 *        -999.000 *
* 12.TDport.M*degc    *           6.693 *          13.662 *        -999.000 *
* 13.TDport.S*degc    *           0.000 *           0.779 *        -999.000 *
* 14.TWstbd.M*degc    *         -18.393 *          13.760 *        -999.000 *
* 15.TWstbd.S*degc    *           0.000 *           5.949 *        -999.000 *
* 16.TDstbd.M*degc    *           6.210 *          14.067 *        -999.000 *
* 17.TDstbd.S*degc    *           0.000 *           0.844 *        -999.000 *
* 18.Sf5/3   *        *           0.001 *           1.551 *        -999.000 *
* 19.truewind*m/s     *           0.463 *          24.107 *        -999.000 *
* 20.seatemp *degc    *          10.008 *          13.000 *        -999.000 *
* 21.modus   *operandi*           1.000 *           3.000 *        -999.000 *
*********************************************************************************
```

Figure 3.18: Pstar header for the file '46avpsd', where 'Sf5/3' is PSD*$F^{5/3}$, and 'truewind' and 'modus' are the outputs from the program *windcors*.

```
DATA DESCRIPTION
****************                    ****************          Prefil:
                          Data Name: *Young      ruCM*         Postfl:
                                     ****************

Even samp:
Archive flag:                              Platform              Depth of  Depth of
Raw data flag: P              **Type** ****Name**** *Number*  instrument  water
Instrument:various            Ship     Cumulus      Cum51         0.00M     0.00M

Fields (Vars):  20    Data cycles:   2492    (2/3D: NROWS:   0    NPLANE:   0)
Start time: 0/     0/000000  Position:  0.0000   0.0000( 0  0.00N   0  0.00E)
*********************************************************************************
*   Field     * Units  *   Lower Limit   *   Upper Limit   * Absent data val *
*********************************************************************************
*  1.jday     *days    *         331.550 *         362.096 *         -999.000 *
*  2.Freq     *Hz      *           0.823 *           0.823 *         -999.000 *
*  3.log10PSD*         *          -6.749 *          -2.030 *         -999.000 *
*  4.VVyng .M*m/s      *           1.639 *          30.160 *         -999.000 *
*  5.DDyng .M*degrees  *          10.733 *         325.810 *         -999.000 *
*  6.DDyng .S*degrees  *           0.387 *         138.178 *         -999.000 *
*  7.PRESS .M*mb       *         953.564 *        1036.517 *         -999.000 *
*  8.PRESS .S*mb       *           0.000 *           6.088 *         -999.000 *
*  9.TWport.M*degc     *          -0.515 *          10.535 *         -999.000 *
* 10.TWport.S*degc     *           0.002 *           0.904 *         -999.000 *
* 11.TDport.M*degc     *           0.199 *          11.318 *         -999.000 *
* 12.TDport.S*degc     *           0.000 *           1.020 *         -999.000 *
* 13.TWstbd.M*degc     *          -1.106 *          10.434 *         -999.000 *
* 14.TWstbd.S*degc     *           0.002 *           0.647 *         -999.000 *
* 15.TDstbd.M*degc     *          -0.092 *          11.109 *         -999.000 *
* 16.TDstbd.S*degc     *           0.003 *           0.962 *         -999.000 *
* 17.Sf5/3    *        *           0.002 *           0.767 *         -999.000 *
* 18.truewind*m/s      *           2.282 *          29.872 *         -999.000 *
* 19.seatemp *degc     *           9.110 *          10.600 *         -999.000 *
* 20.modus   *operandi*           1.000 *           3.000 *         -999.000 *
*********************************************************************************

Comment:
 1:modus operandi:
 2:1 = Bow winds > 12 m/s
 3:2 = Port winds < 17 m/s
 4:3 = Other
 5:Absent = Steaming (found from ship's log)
```

Figure 3.19: As Fig 3.18 but for the file '51avpsd'.

```
DATA DESCRIPTION
****************                    ****************          Prefil:
                          Data Name: *MultiMet  ruZB*          Postfl:
                                     ****************
Even samp:
Archive flag:                              Platform              Depth of  Depth of
Raw data flag: P                 **Type** ****Name**** *Number*  instrument  water
Instrument:                                                         0.00M     0.00M

Fields (Vars):  36    Data cycles:   2055    (2/3D: NROWS:   0   NPLANE:   0)
Start time: 1/870000/000000  Position:  0.0000   0.0000( 0  0.00N   0  0.00E)
*********************************************************************************
*   Field    * Units  *   Lower Limit   *   Upper Limit   * Absent data val *
*********************************************************************************
*  1.jday    *days    *         277.708 *         305.198 *        -999.000 *
*  2.SERIALno*        *          38.000 *          38.000 *        -999.000 *
*  3.        *        *          96.000 *          96.000 *        -999.000 *
*  4.min freq*Hertz   *           2.000 *           2.000 *        -999.000 *
*  5.max freq*Hertz   *           4.000 *           4.000 *        -999.000 *
*  6.Mode    *        *           1.000 *           1.000 *        -999.000 *
*  7.MEAN SPD*M/S     *           1.240 *          24.650 *        -999.000 *
*  8.MEANNSPD*M/S     *         -22.010 *          13.180 *        -999.000 *
*  9.MEANESPD*M/S     *          -4.810 *          23.000 *        -999.000 *
* 10.MEANVSPD*M/S     *          -0.210 *           3.870 *        -999.000 *
* 11.SP SOUND*M/S     *         336.620 *         367.600 *        -999.000 *
* 12.unlogPSD*        *           0.000 *           0.669 *        -999.000 *
* 13.Coeff A *        *           0.001 *           0.695 *        -999.000 *
* 14.COEFF B *10**-8  *   -1971070.000 *     1733600.000 *        -999.000 *
* 15.psd/cfA *        *           0.700 *           1.300 *        -999.000 *
* 16.wspeed  *m/s     *           1.048 *          23.609 *        -999.000 *
* 17.wdir    *deg     *           0.091 *         359.683 *        -999.000 *
* 18.jday  .M*days    *         277.712 *         305.201 *        -999.000 *
* 19.jday  .S*days    *           0.002 *           0.002 *        -999.000 *
* 20.PRESS .M*mb      *         988.832 *        1034.096 *        -999.000 *
* 21.PRESS .S*mb      *           0.000 *           0.779 *        -999.000 *
* 22.TDport.M*degc    *           4.016 *          12.157 *        -999.000 *
* 23.TDport.S*degc    *           0.002 *           1.068 *        -999.000 *
* 24.TWport.M*degc    *           2.298 *          11.772 *        -999.000 *
* 25.TWport.S*degc    *           0.002 *           0.527 *        -999.000 *
* 26.TDstbd.M*degc    *           4.326 *          12.501 *        -999.000 *
* 27.TDstbd.S*degc    *           0.002 *           1.041 *        -999.000 *
* 28.TWstbd.M*degc    *           1.883 *          11.994 *        -999.000 *
* 29.TWstbd.S*degc    *           0.002 *           0.457 *        -999.000 *
* 30.truewind*m/s     *           1.700 *          22.909 *        -999.000 *
* 31.modus   *operandi*           1.000 *           3.000 *        -999.000 *
* 32.sst     *deg     *          10.400 *          11.900 *        -999.000 *
* 33.vspd    *m/s     *           1.051 *          23.673 *        -999.000 *
* 34.tilt    *deg     *          72.574 *          92.631 *        -999.000 *
* 35.vtrue   *m/s     *           1.729 *          23.102 *        -999.000 *
*********************************************************************************
```

Figure 3.20: Pstar header for the file 'cleanvtrue' where 'unlogPSD' is PSD*$F^{5/3}$, 'wspeed' is the relative wind speed calculated from East and North components, 'vspd' is the relative wind speed calculated from the East, North and Vertical components, 'truewind' and 'modus' are from the program *windcors* using the E/N relative wind, and 'vtrue' is the true wind calculated from the E/N/V relative wind.

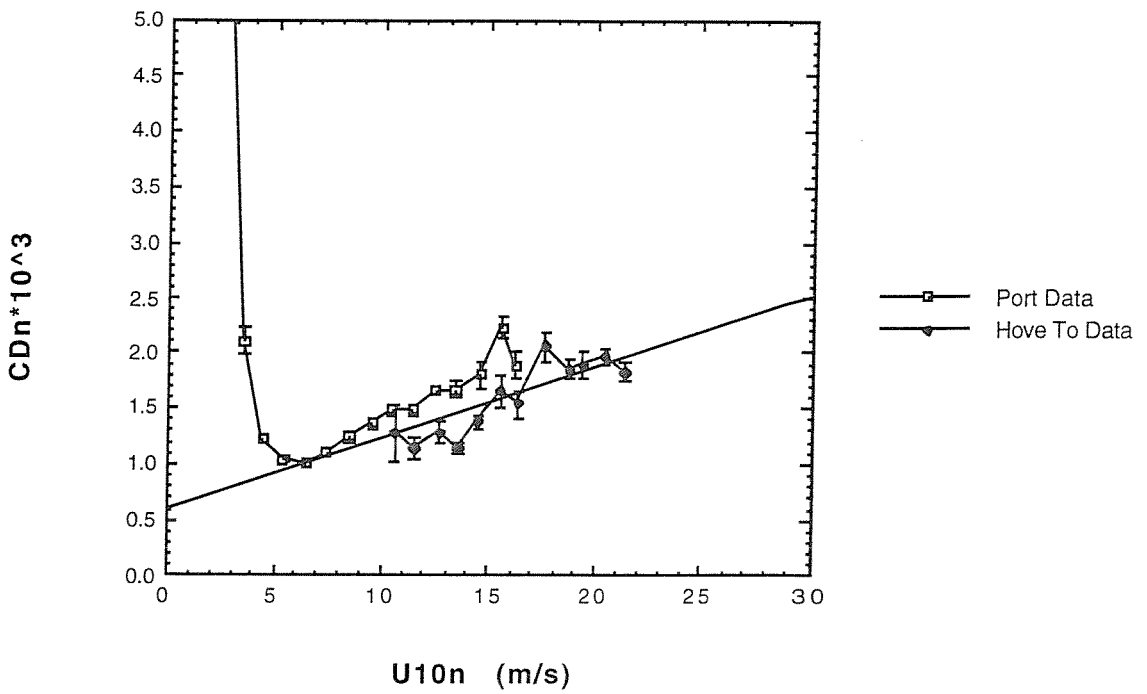

Figure 3.21: Neutral Drag Coefficient against 10 metre wind speed for Cruise 46 data. The solid line is the Smith (1980) relationship.

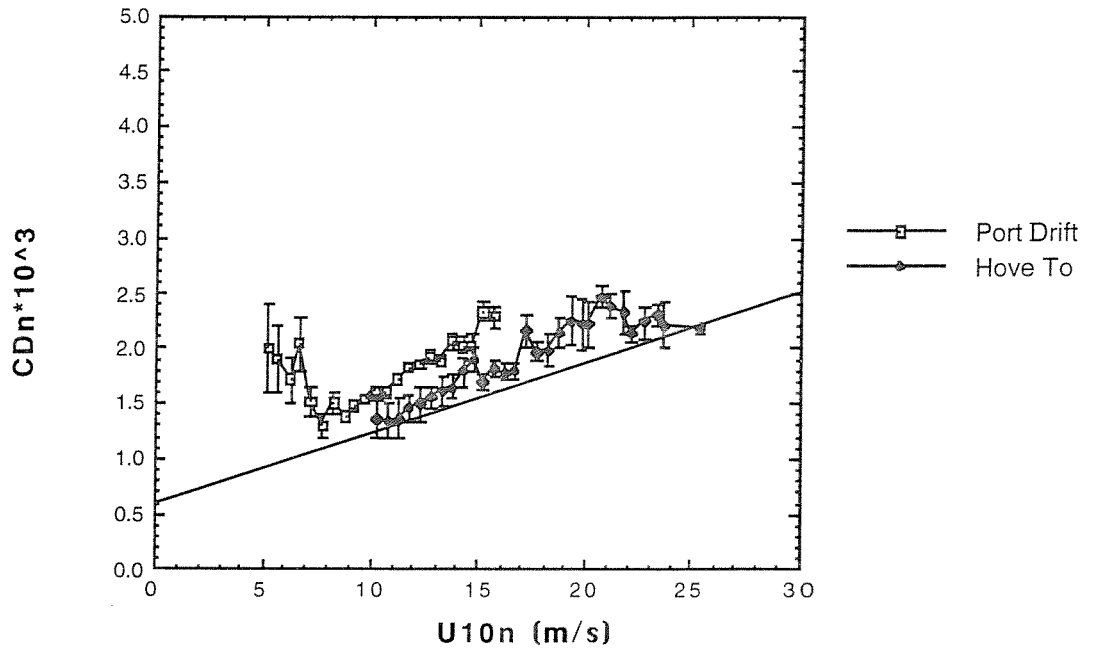

Figure 3.22: As Fig 3.21 except for Cruise 51 data.

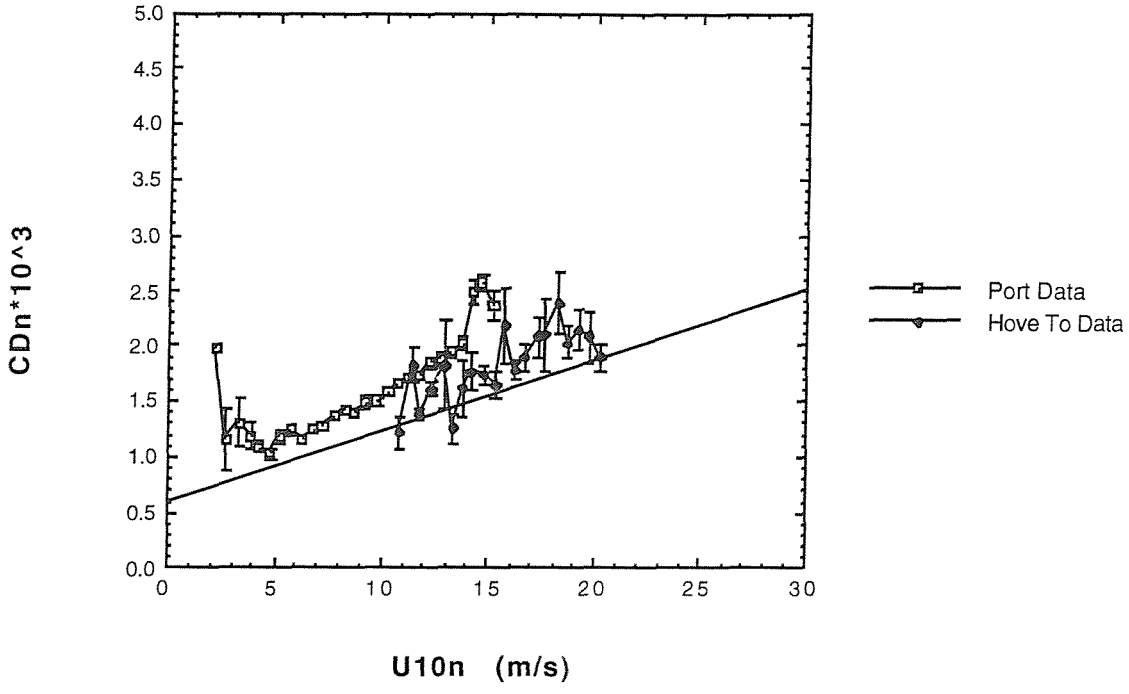

Figure 3.23: As Fig 3.21 except for Cruise 70 data.

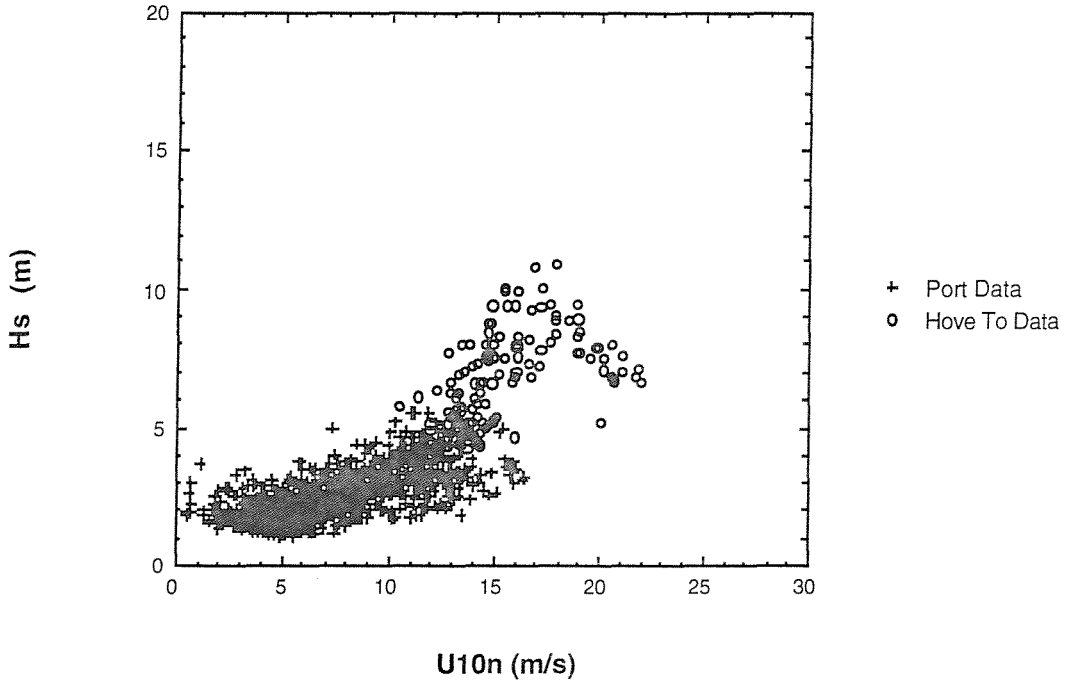

Figure 3.24: Significant wave height against 10 metre wind speed for Cruise 46 data. The crosses show data from when the ship was drifting, the circles show hove to data.

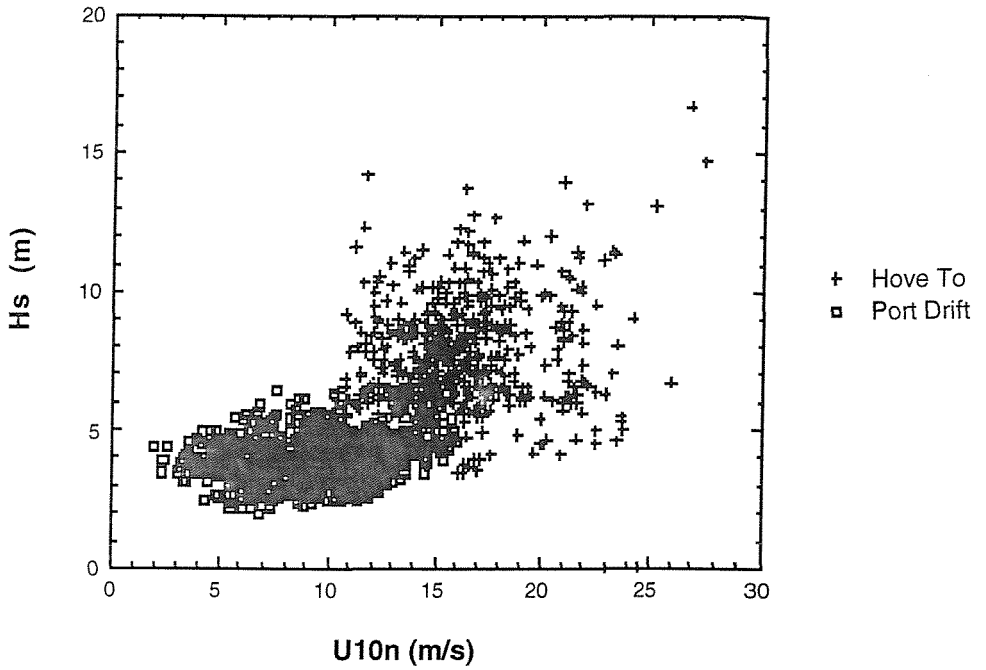

Figure 3.25: Significant wave height against 10 metre wind speed for Cruise 51 data. The squares show data from when the ship was drifting, the crosses show hove to data.

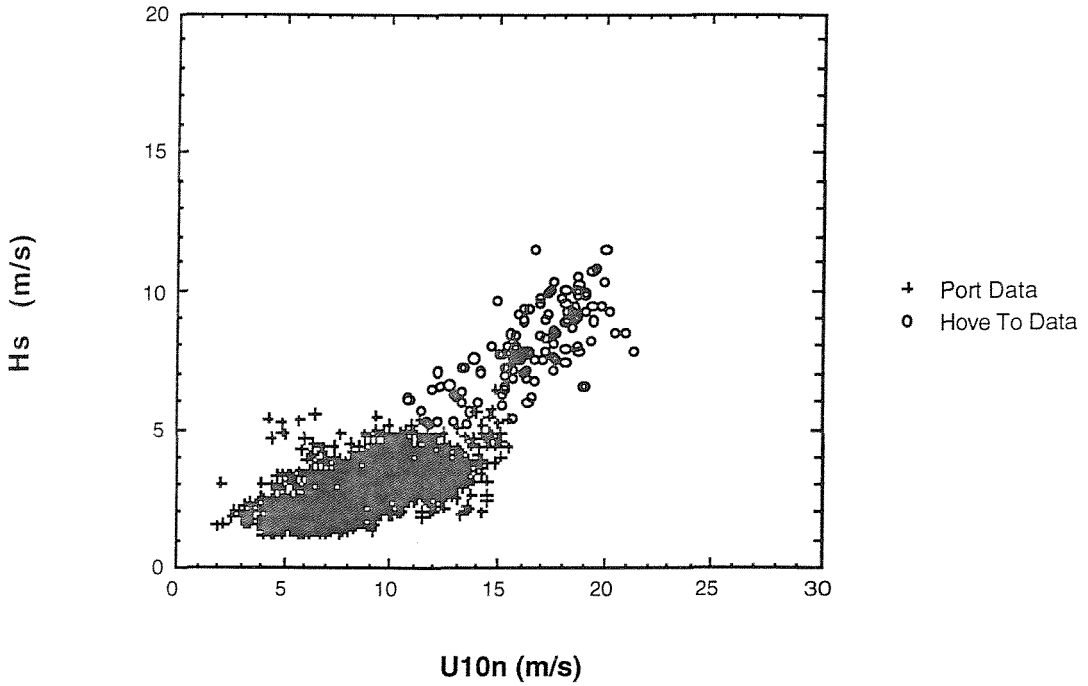

Figure 3.26: Significant wave height against 10 metre wind speed for Cruise 70 data. The crosses show data from when the ship was drifting, the circles show hove to data.

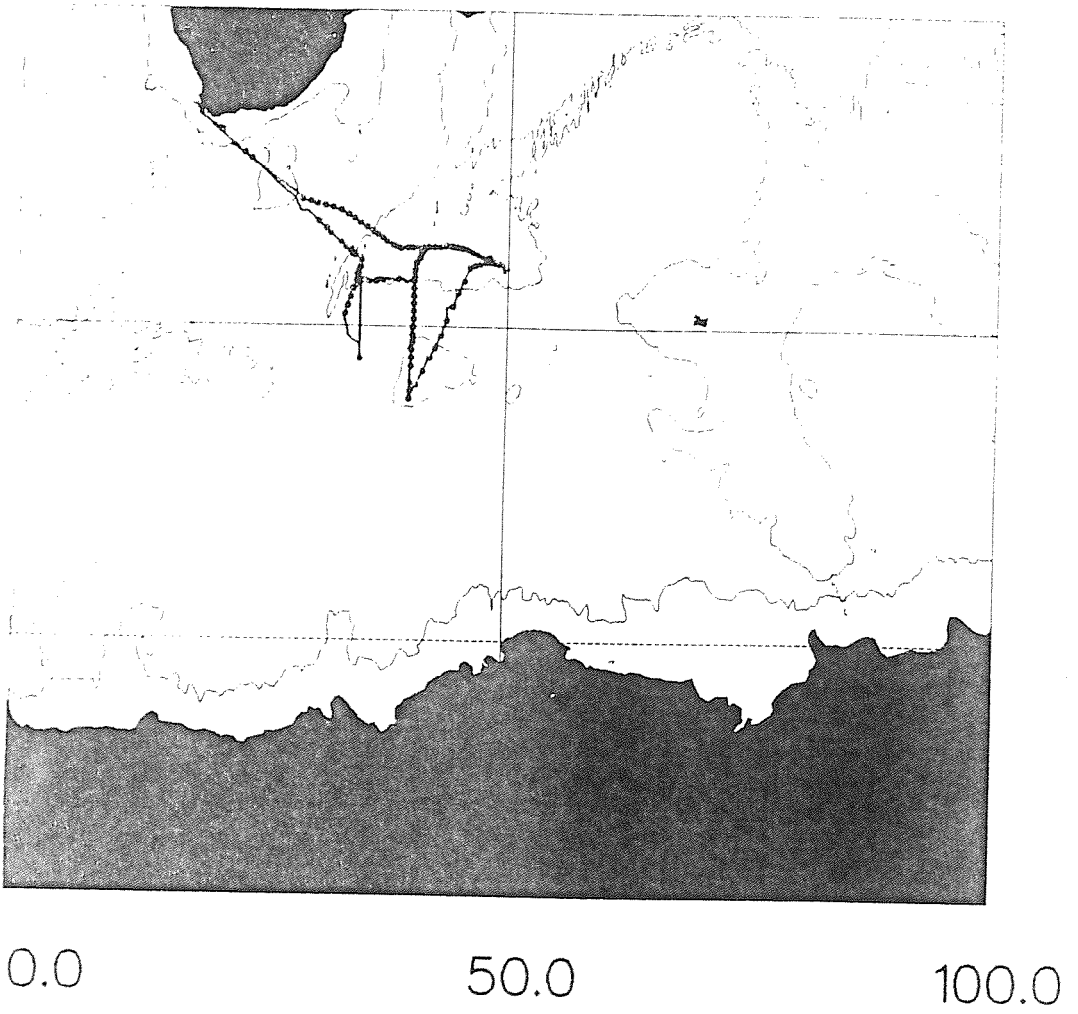

Figure 4.1: The track of the R.R.S. Discovery SWINDEX cruise.

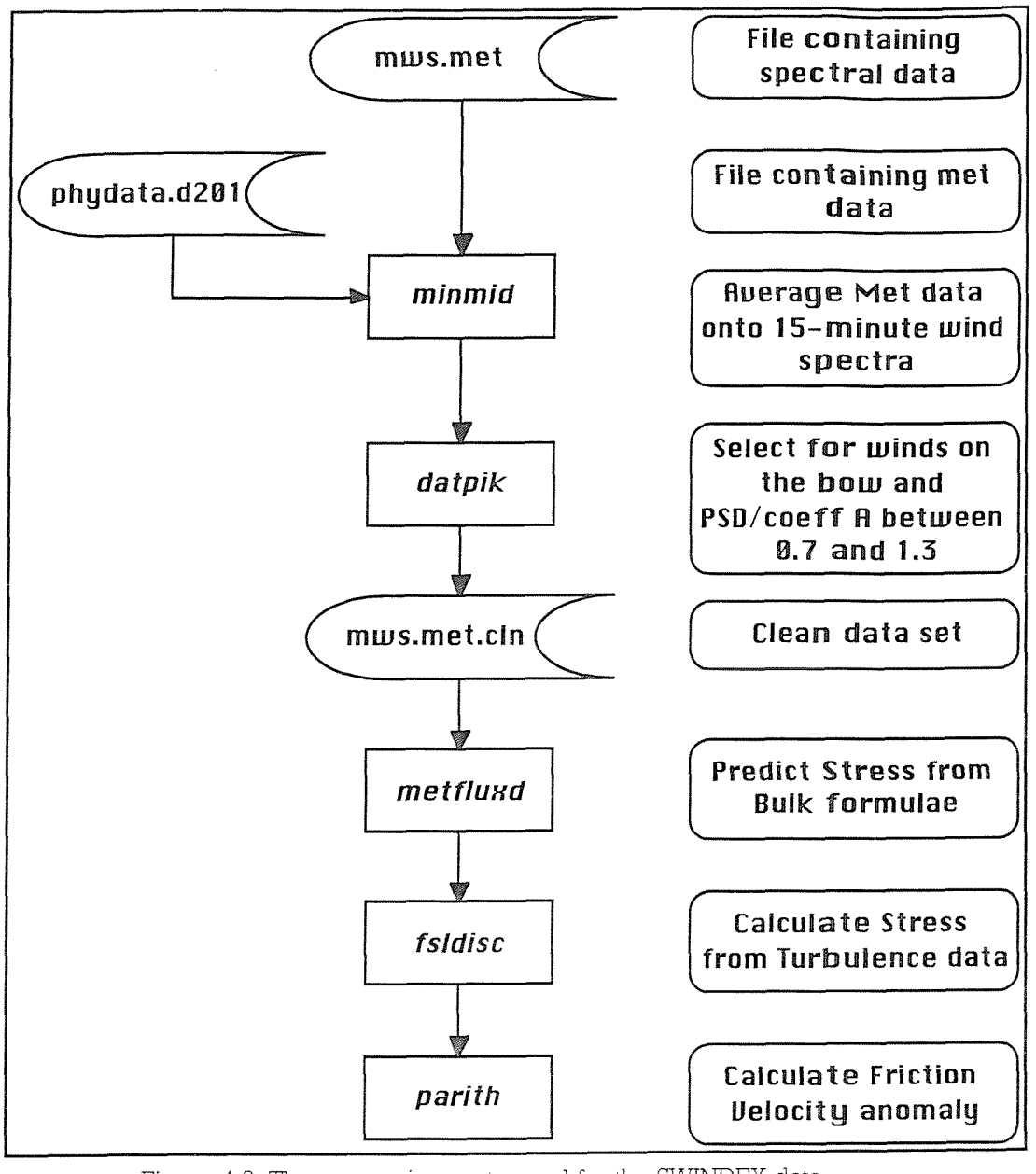

Figure 4.2: The processing route used for the SWINDEX data.

```
DATA DESCRIPTION
****************                    ****************          Prefil:
                          Data Name: *mm201tru  ruOG*          Postfl:
                                     ****************

Even samp:30       Seconds
Archive flag: N                        Platform              Depth of  Depth of
Raw data flag: P              **Type** ****Name**** *Number*  instrument  water
Instrument:                                                      0.00M     0.00M

Fields (Vars):  39    Data cycles:   1388    (2/3D: NROWS:   0   NPLANE:   0)
Start time:19/930101/000000  Position:  0.0000   0.0000( 0  0.00N   0  0.00E)
*********************************************************************************
*   Field    * Units  *   Lower Limit   *   Upper Limit   * Absent data val *
*********************************************************************************
*  1.JDAY    *DAYOFYR *          82.698 *         120.729 *        -999.000 *
*  2.Mode    *        *           1.000 *           4.000 *        -999.000 *
*  3.MEAN SPD*M/S     *           0.780 *          28.280 *        -999.000 *
*  4.MEANNSPD*M/S     *           0.590 *          24.120 *        -999.000 *
*  5.MEANESPD*M/S     *         -18.720 *          15.120 *        -999.000 *
*  6.MEANVSPD*M/S     *           0.030 *           3.100 *        -999.000 *
*  7.PSD     *        *           0.000 *           0.647 *        -999.000 *
*  8.cofA    *        *           0.000 *           0.697 *        -999.000 *
*  9.jday  .M*dayofyr *          82.701 *         120.733 *        -999.000 *
* 10.jday  .S*dayofyr *           0.002 *           0.002 *        -999.000 *
* 11.windsp.M*m/s     *           0.697 *          26.788 *        -999.000 *
* 12.windsp.S*m/s     *           0.056 *           3.446 *        -999.000 *
* 13.winddi.M*bow=180 *         120.562 *         239.830 *        -999.000 *
* 14.winddi.S*bow=180 *           0.392 *          19.996 *        -999.000 *
* 15.swette.M*degc    *          -0.610 *          19.984 *        -999.000 *
* 16.swette.S*degc    *           0.002 *           0.714 *        -999.000 *
* 17.sdryte.M*degc    *           1.574 *          27.235 *        -999.000 *
* 18.sdryte.S*degc    *           0.002 *           1.091 *        -999.000 *
* 19.seatem.M*degc    *           2.499 *          25.338 *        -999.000 *
* 20.seatem.S*degc    *           0.000 *           1.564 *        -999.000 *
* 21.baro  .M*mb      *         980.590 *        1029.630 *        -999.000 *
* 22.baro  .S*mb      *           0.000 *           0.336 *        -999.000 *
* 23.truews.M*m/s     *           0.410 *          26.532 *        -999.000 *
* 24.truews.S*m/s     *           0.035 *           2.443 *        -999.000 *
* 25.pfa   .M*m/s     *          -0.373 *           7.072 *        -999.000 *
* 26.pfa   .S*m/s     *           0.000 *           2.307 *        -999.000 *
* 27.pps   .M*m/s     *          -0.535 *           1.082 *        -999.000 *
* 28.pps   .S*m/s     *           0.000 *           0.324 *        -999.000 *
* 29.vvtrue.M*em      *           0.742 *          25.849 *        -999.000 *
* 30.vvtrue.S*em      *           0.064 *           3.447 *        -999.000 *
* 31.pgyro .M*degrees *           2.488 *         359.303 *        -999.000 *
* 32.pgyro .S*degrees *           0.027 *         172.018 *        -999.000 *
* 33.SSrel   *m/s     *           0.633 *          28.125 *        -999.000 *
* 34.SSddrel *bow=180 *         121.059 *         245.230 *        -999.000 *
* 35.SSN-pfa *m/s     *          -5.664 *          23.189 *        -999.000 *
* 36.SSE-pps *m/s     *         -19.802 *          15.058 *        -999.000 *
* 37.SStru em*m/s     *           0.604 *          27.171 *        -999.000 *
* 38.SStrudd *degrees *           0.779 *         359.985 *        -999.000 *
* 39.PSD/cofA*        *           0.703 *           1.299 *        -999.000 *
*********************************************************************************
```

Figure 4.3: Pstar header of the file 'mws.met.cln', where 'SStru em' is the true wind as calculated from the relative wind and em log data, 'PSD' is $PSD*F^{5/3}$ and 'PSD/cofA' is the ratio of $PSD*F^{5/3}$ to the intercept of the spectrum.

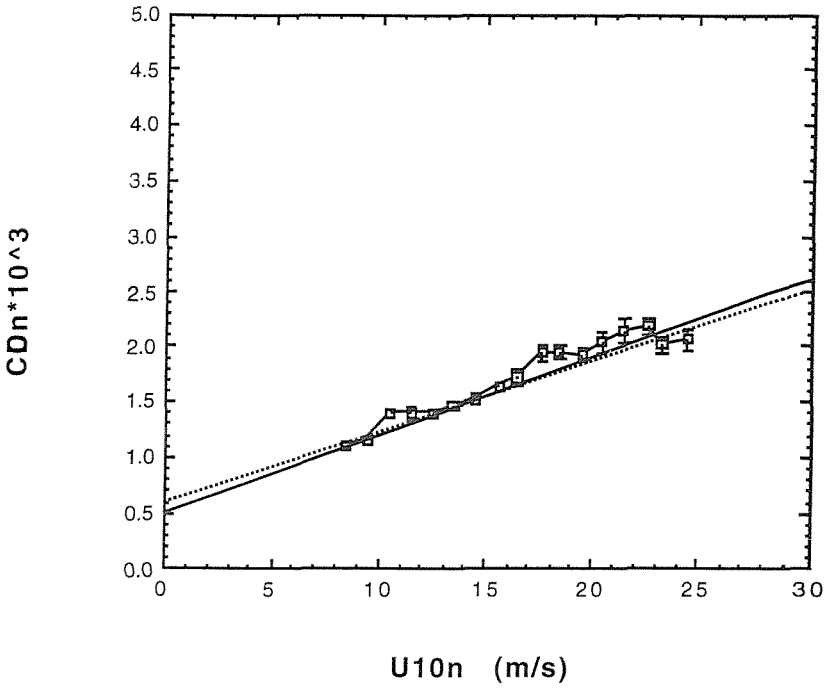

Figure 4.4: Neutral Drag Coefficient against 10 metre wind speed for Discovery cruise 200 data. The dashed line shows the Smith (1980) relationship, the solid line show a least squares fit to the data.

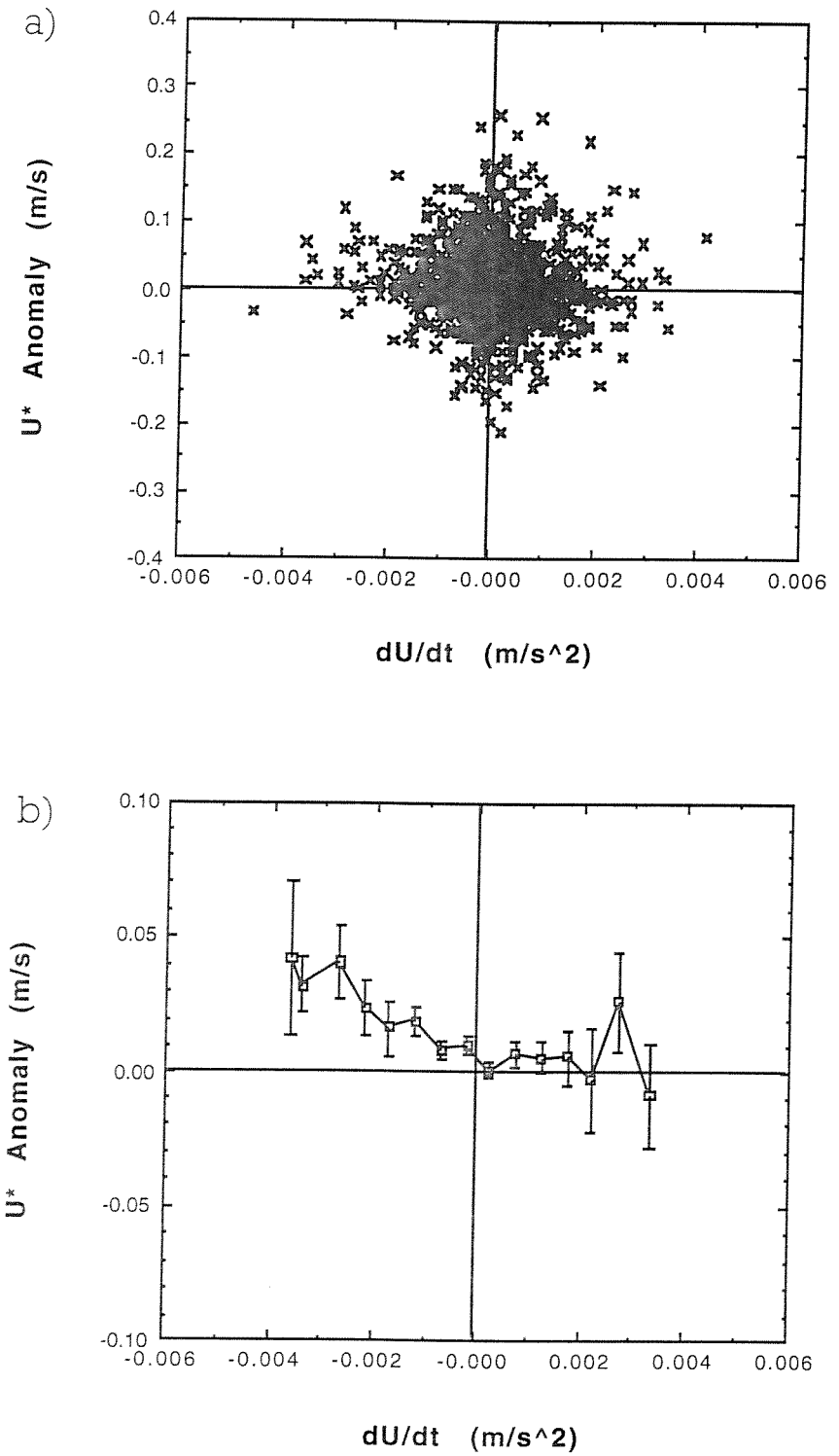

Figure 4.5: Rate of change 15-minute mean wind speed with time against U* anomaly. Fig a) shows the data as a scatter plot, Fig b) shows the data binned on dU/dt.

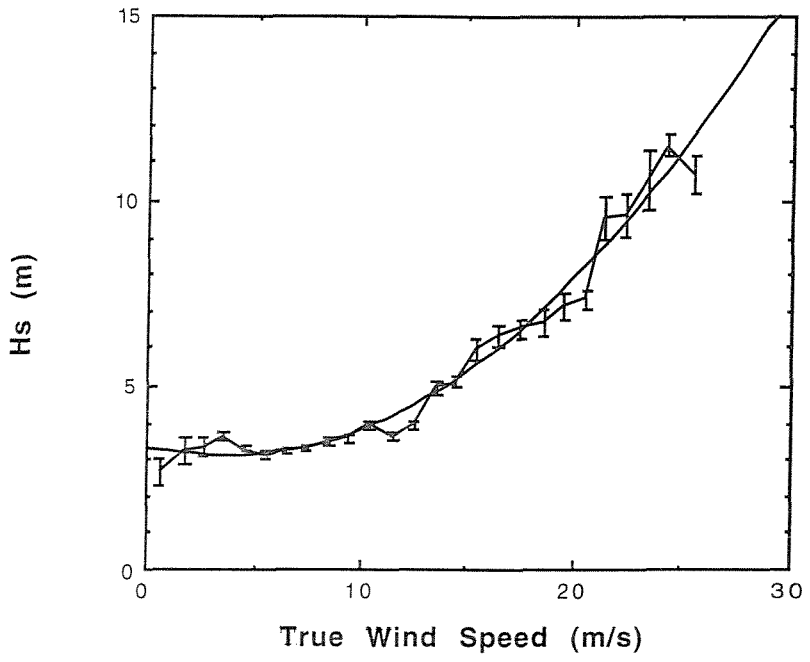

Figure 4.6: Significant wave height against true wind speed for SWINDEX data. The equation of the line of best fit is Hs = 3.32 - 0.136 U + 0.0181 U^2.

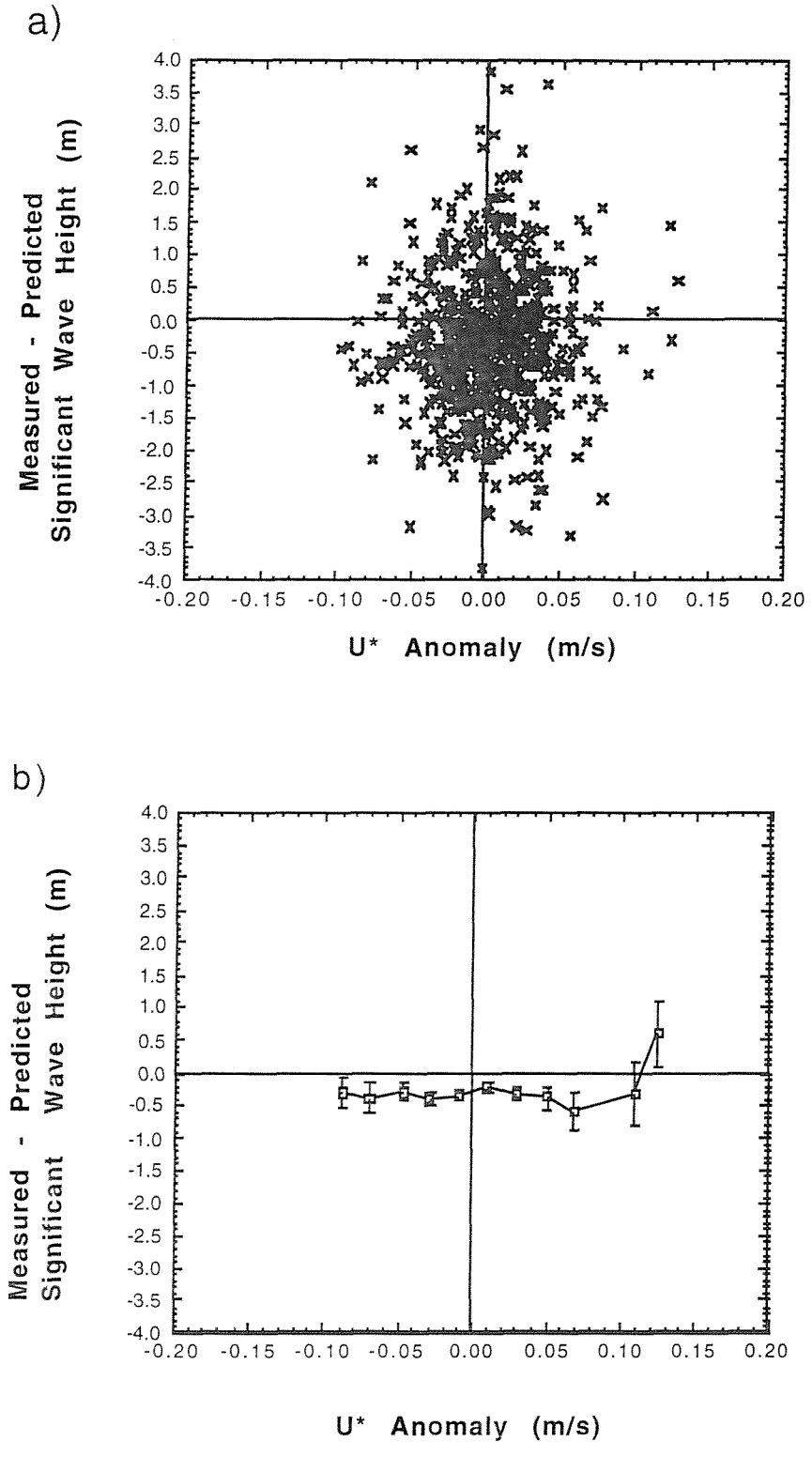

Figure 4.7: Significant wave height anomaly against U* anomaly for SWINDEX data. Fig b) shows the data binned on U* anomaly.

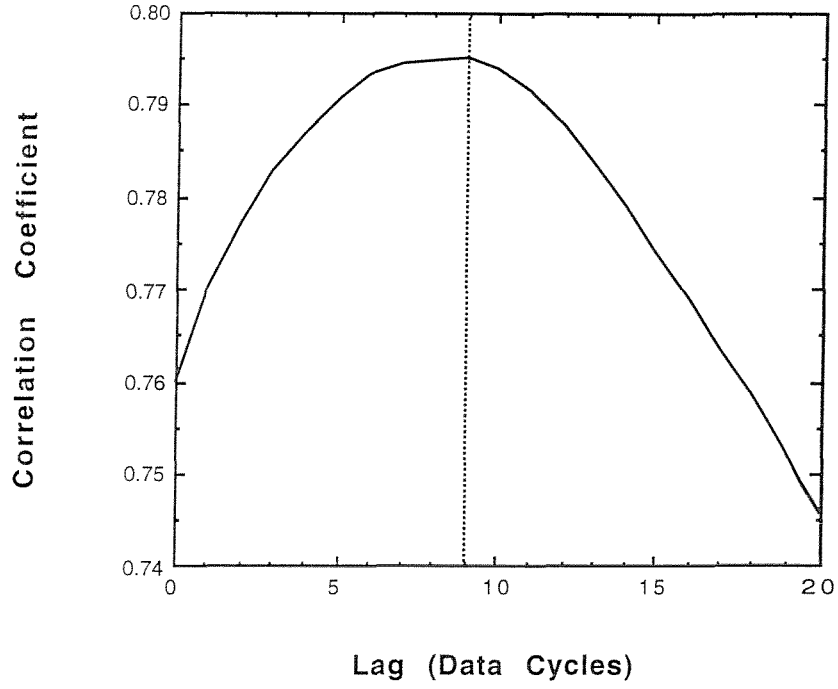

Figure 4.8: Correlation coefficient against time lag (in data cycles) from the program *pcorr*.

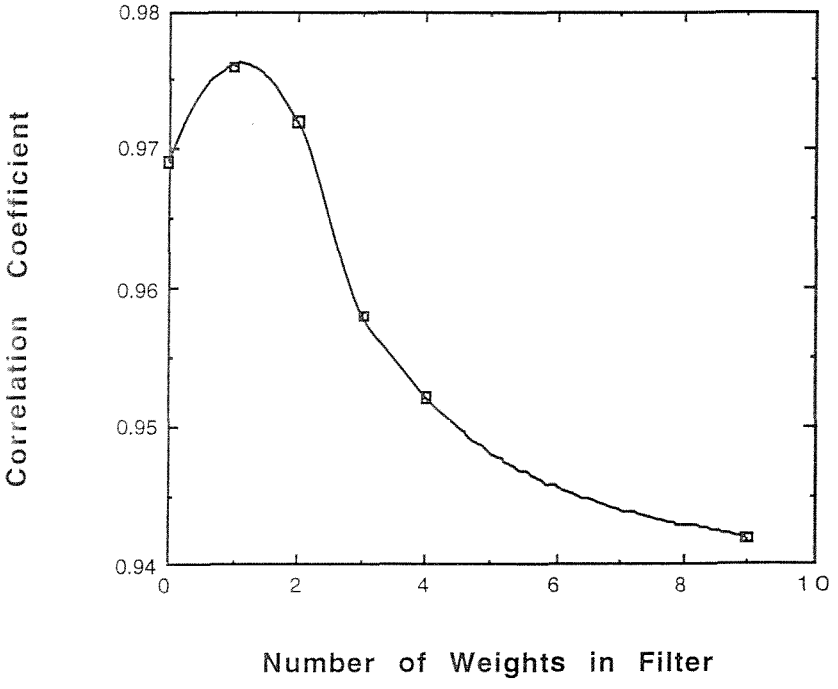

Figure 4.9: Correlation coefficient of quadratic fit to data against width of filter used on wind speed data.

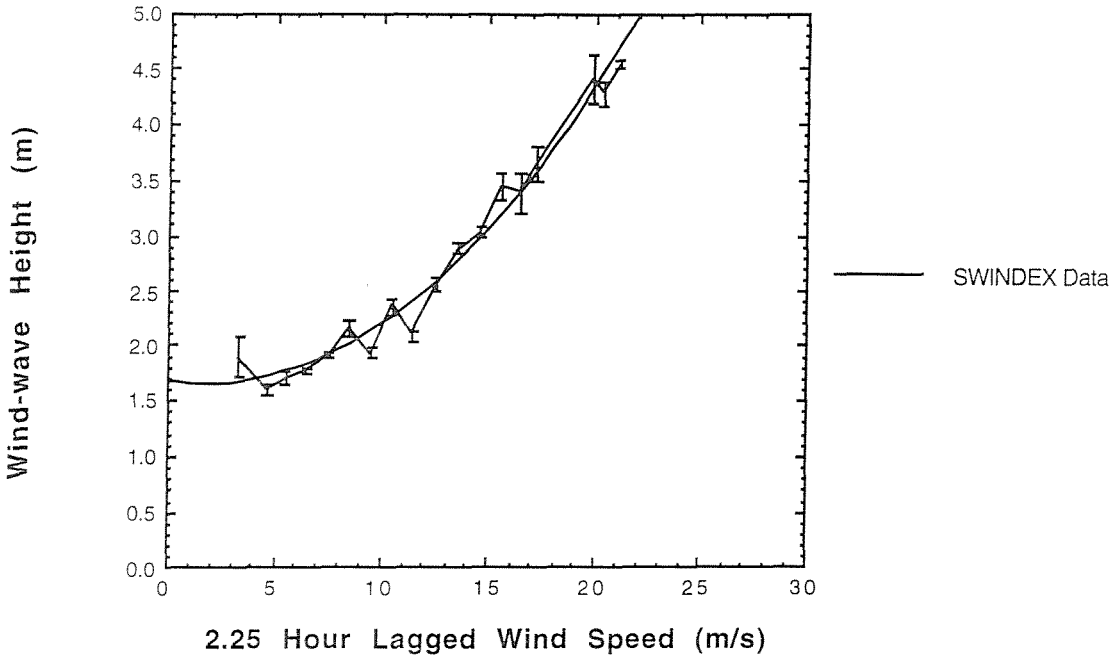

Figure 4.10: Wind wave height against wind speed, lagged by 2.25 hours and filtered using 3-point width top hat filter.

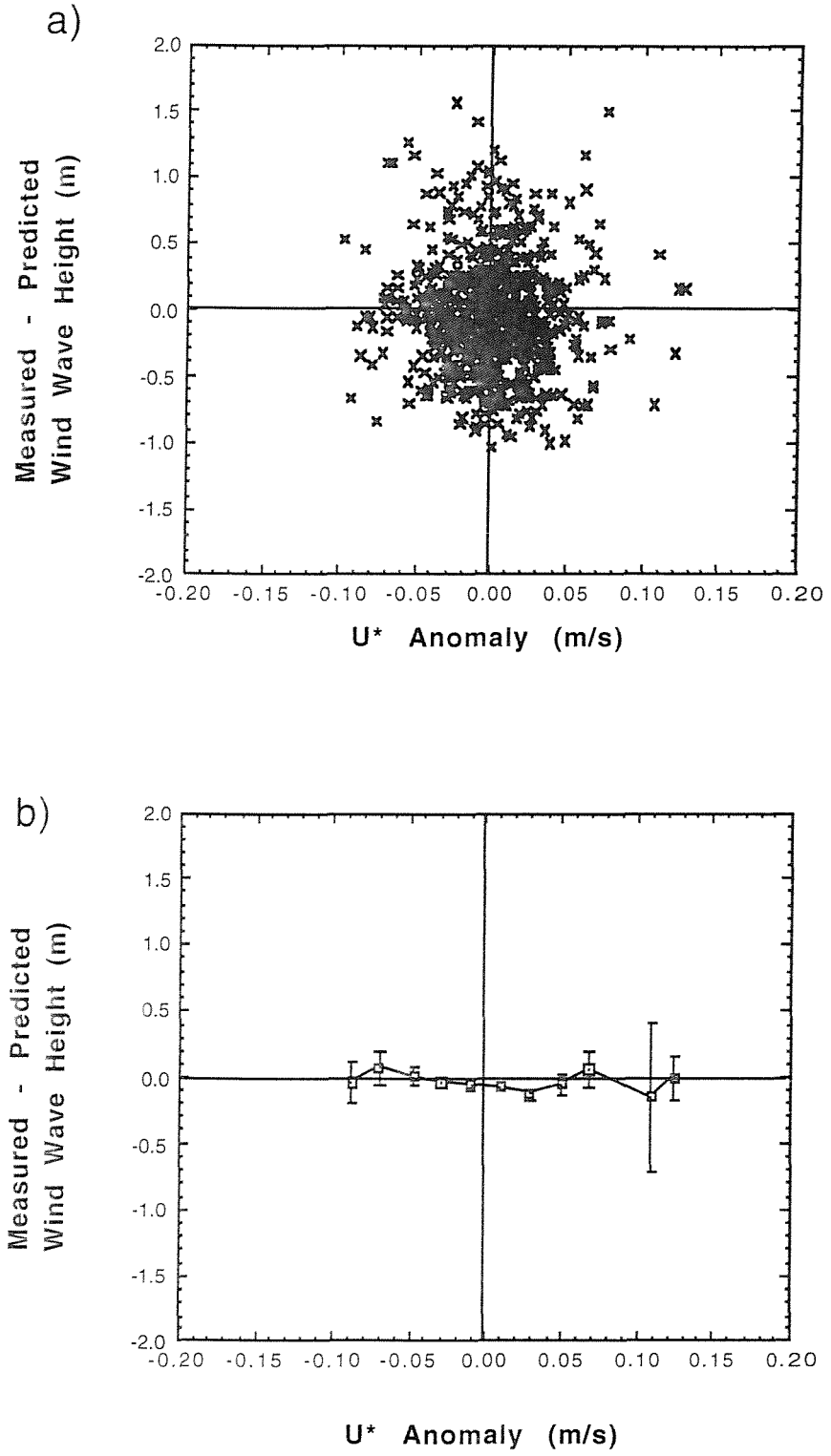

Figure 4.11: Wind wave height anomaly against U* anomaly. Fig b) shows the data binned on U* anomaly.


Natural
Environment
Research
Council